THE HEATING OF THE SOLAR CHROMOSPHERE, PLAGES, AND CORONA BY MAGNETOHYDRODYNAMIC WAVES

DONALD E. OSTERBROCK*
Institute for Advanced Study, Princeton, New Jersey
Received April 10, 1961; revised May 10, 1961

ABSTRACT

The energy radiated from the chromosphere, the corona, and the upper chromosphere is approximately estimated from observational data. The energy carried upward by sound waves generated in the hydrogen convection zone is estimated and found sufficient to balance these losses, though the numerical result is highly uncertain because of its great dependence on the turbulent velocity field The spectrum of this noise is a broad band with maximum near the frequency of 0 01 cps. The waves propagate in the so-called "fast" mode and become increasingly magnetohydrodynamic in character as they run out through the chromosphere, because of the negative density gradient. Little, if any, energy is emitted by the hydrogen convection zone in the "slow" or "Alfvén" modes, and these modes are, in addition, strongly absorbed in the photosphere. The cross-sections for collisions between neutral atoms and ions in the chromosphere is large, and, as a result, the dissipation of the fast-mode waves by the frictional damping mechanism is very small. The waves build up to shocks, and the dissipation of these shocks is the main energy source for the chromosphere The dissipation of the shocks is worked out by using a similarity principle, in a way analogous to the Brinkley-Kirkwood theory of the dissipation of pure gas-dynamic shocks At great heights, where the magnetic field dominates, the shocks become weaker, the dissipation decreases, and the rays are refracted back downward toward the photosphere. However, at these heights, collisions between shocks must be expected to feed some energy into the slow mode and the Alfvén mode, and these modes then propagate straight up the magnetic line of force, with essentially no weakening by refraction, and carry energy into the corona. The plages are regions of larger magnetic field, where there is extra generation of noise in the hydrogen convection zone below and where the refraction and shock-collision effects are more important. The spicules seen at the limb of the sun are interpreted as slow-mode disturbances carrying chromospheric material up along the magnetic lines of force into the corona.

I. INTRODUCTION

It has been known for some years that near the visible surface of the sun the temperature gradient becomes zero and that in the chromosphere and corona the temperature (defined by the average microscopic kinetic energy of the material particles) increases outward. The physical explanation of this phenomenon was given independently by Schwarzschild (1948) and Biermann (1948), who showed that it is due to the dissipation of shock waves. These disturbances are generated as small-amplitude sound waves by the turbulence in the hydrogen convection zone and propagate outward, increasing in amplitude because of the decreasing density they encounter in the solar atmosphere, until they build up to shocks, and then are rapidly dissipated. The small fraction of the sun's energy carried by the waves is transported in this way through the photosphere and reversing layer and is liberated farther out, in the chromosphere and corona. These outer layers thus come to a temperature set by the balance between the energy supplied to them by the waves and the energy radiated from them as light. These ideas were worked out in a detailed way by Schatzman (1949) and by Schirmer (1950), who showed that many of the observed features of the chromosphere and corona could be understood through them.

However, beginning with Alfvén (1947), many authors (van de Hulst 1953; Piddington 1956; De Jager 1959*a*) have emphasized that, since the solar atmosphere is a partly ionized gas in which there is a non-zero magnetic field, the electromagnetic forces may be expected to have some importance in the generation, propagation, and dissipation of

* John Simon Guggenheim Post-doctoral Fellow on leave of absence from the University of Wisconsin.

the waves. The most direct evidence of the correctness of this view is provided by the observational results (Babcock and Babcock 1958; Howard 1959; Leighton 1959) that the calcium plages, which are regions where the chromospheric K emission line of Ca II is exceptionally bright, exactly coincide with the regions of strong magnetic field. Thus there is observed, in these regions, enhanced heating apparently directly caused by magnetic fields.

Another indication of the importance of magnetic fields in the heating of the outer layers of the sun is provided by the spicules (Roberts 1945) or jets (Mohler 1951) observed at the limb in the upper chromosphere. These features have been considered by many authors (Thomas 1948; van de Hulst 1953) to be visible examples of shock waves propagating out from the chromosphere and dissipating in the corona, but their direction corresponds quite closely with the direction of the solar magnetic field, as indicated by the coronal rays (van de Hulst 1958). This can be seen especially clearly in the comparison of the appearance of the corona at the eclipse of June 30, 1954 (Gold 1955), very close to sunspot minimum, with the mean directions of the spicules about a year later, still close to, but not exactly at, sunspot minimum (Lippincott 1957). It is also known that

TABLE 1

CA II 3933 EMISSION LINE IN MAIN-SEQUENCE STARS

Star	Classification	Line Width (km/sec)	Line Intensity*
κ Cet	G5 V	48	3
σ^2Eri A	(K0 V)†	47	2
61 U Ma	G8 V	50	3
ξ Boo br	G8 V	46	5
70 Oph br	K0 V	48	3
σ Dra	K0 V	50	1
16 Cyg foll.	G5 V		0

* Intensity scale: 0 = invisible; 5 ≳ continuum

† Spectral type estimated from trigonometric absolute magnitude

spicules close to coronal arches depart from the radial direction and lie in the direction tangent to the arches (Rush and Roberts 1954). Thus there appears to be a close connection between the solar magnetic field and the outward-propagating disturbances in the upper chromosphere.

Another more indirect indication of the importance of magnetic fields in the heating of the chromosphere is provided by observations of the K emission lines in the spectra of late-type stars. Though the surface structure cannot be resolved in any of these stars, it seems clear that the emission line must arise in an outer chromosphere, as in the sun. The observational results (Wilson and Bappu 1957) show that the width of the K emission line is completely fixed by the luminosity of the star but that the strength or intensity of the line is not fixed by the spectral type and luminosity. This is illustrated in Table 1, where the widths and intensities are given for the Ca II emission lines in the spectra of all the dwarf stars observed by Wilson and Bappu (1957) in the interval G5–K0. The wide range of intensities shown in this table could not occur if the chromospheric heating in these stars depended only on the dissipation of pure gas-dynamic waves, because, according to the Russell-Vogt theorem (see, e.g., Chandrasekhar 1938), the whole structure of a star, including the properties of its hydrogen convection zone, depend only on its mass and composition, and there should therefore be a unique correlation between spectral type and luminosity, on the one hand, and chromospheric structure and resulting K-line intensity, on the other. However, we can easily imagine that the stars differ

among themselves in magnetic-field strength and distribution, probably as a result of the conditions in the gas clouds from which they formed (Cowling 1945; Spitzer 1958), and therefore the observed differences in chromospheric properties can be understood if the heating mechanism depends on magnetic effects (Leighton 1959).

From a theoretical point of view, it is clear that magnetohydrodynamic effects must become important at some height in the chromosphere, because the velocity of sound V_S is, to a first approximation, constant, while the Alfvén-wave velocity $V_A = B/(4\pi\rho)^{1/2}$ increases rapidly outward, because of the outward decrease in density. The magnetic effects are small when $V_A < V_S$ but cannot be neglected when $V_A > V_S$; the condition $V_A = V_S$ holds at a height of 2000 km with an assumed field strength $B = 2$ gauss and the density distribution tabulated by van de Hulst (1953), but, because of the steep density gradient, the conclusion that the equality is satisfied somewhere in the chromosphere applies over a very wide range of models.

The present paper is therefore concerned with the generation, propagation, and dissipation of the magnetohydrodynamic waves that heat the outer layers of the sun. The actual structure of these layers, as derived from observational data, is not at all well known; in addition, the theory of magnetohydrodynamic waves has not yet been completely worked out, and those parts that have been are in many cases mathematically quite complicated. For these reasons their treatment in the present paper is approximate and highly schematic and is aimed chiefly at isolating the important physical processes for further detailed study rather than at providing a complete and final picture of the chromosphere and corona. It is intended to be a critical synthesis of separate ideas originally proposed by many individual authors.

We first discuss the relevant observational material for the sun and then describe briefly the magnetohydrodynamic-wave modes that can occur in an ionized gas in a magnetic field. Next the generation of the waves in the hydrogen convection zone is treated in a more detailed way, and it is shown that the energy produced is about the correct amount to balance the observed radiative losses. This energy propagates outward in the fast mode; little, if any, energy is emitted by the hydrogen convection zone in the Alfvén or slow modes, and these modes are, in addition, shown to be strongly absorbed by the Piddington frictional process in the photosphere. However, this mechanism is shown to play little part in damping the fast-mode waves in the chromosphere, which, instead, build up to finite-amplitude shocks and then are dissipated. It is shown quantitatively that this shock dissipation begins at approximately the observed level in the solar atmosphere, that is, that the wave energy largely passes through the photosphere and reversing layer with little damping and that the shock dissipation provides approximately the correct amount of heating for the lower chromosphere. At greater heights, where the magnetic field dominates, it is shown that the shocks become weaker and that the fast-mode waves are refracted back down toward the photosphere and that, for both these reasons, the dissipation decreases rapidly. However, it is shown qualitatively (but not quantitatively) that some energy must be fed into the slow and Alfvén modes in the chromosphere and that the dissipation of these waves, which travel upward along the lines of force without refraction, is probably responsible for heating the uppermost part of the chromosphere and the corona. The spicules observed at the limb of the sun are, on this picture, slow-mode disturbances propagating upward, but some difficulties remain, particularly in the heights to which they reach. The plages can be understood as regions of larger magnetic field, where the wave generation in the hydrogen convection zone below is probably larger and where refraction and shock collisions in the chromosphere are more important, both of these effects leading to greater heating.

II. OBSERVATIONAL DATA

In principle, if all the relevant physical processes were known, it should be possible to calculate the entire structure of the chromosphere and corona, beginning with only a few

solar parameters, such as the flux of energy in the form of acoustical waves incident from below, the acceleration of gravity, etc. However, at the present time, much of the theory, though known in outline, remains incompletely worked out, and it seems preferable to base our discussion as much as possible on the observed properties of the outer layers of the sun. Thus, in all the calculations reported here, the table of density, temperature, and degree of ionization as functions of height given by van de Hulst (1953) has been used as defining the average properties of the chromosphere. It is based on the analysis and interpretation of large amounts of observational data obtained by many investigators, and considerable selection and judgment are involved; for this reason, we cannot trust those parts of the results of the present paper that depend in a detailed way on the temperature or density distribution, but, in fact, all the main results are invariant to a change to any reasonable model chromosphere. Now it must be understood that at any particular height in the chromosphere there are pronounced fluctuations in temperature, density, etc., and the values listed in the table are only average values that represent a first approximation to the structure; the next higher approximation is a two-element model with hot and cold elements at each height (see Woltjer 1954; Athay and Menzel 1956; De Jager 1957), while the true structure involves a continuum of temperatures and density at each height. As will be seen below, particularly in Sections VII and VIII in this paper, the lower temperature of the two-element approximation, which corresponds fairly well to the single temperature of van de Hulst's model, is regarded as being a property of the relatively undisturbed chromosphere ahead of a shock wave, while the high temperature is regarded as applying to the overheated material behind the shock or in the region in which two shocks have just collided.

The main data needed for checking the results of the present paper are the amounts of energy radiated from the outer layers of the sun, as a function of height, because this radiation balances the heating we are considering. However, the energy radiated from the chromosphere cannot be observed directly, because the bulk of the chromospheric light received at the earth is actually light emitted in the photosphere and reversing layer and has simply been scattered by resonance fluorescence in the chromosphere (Wurm 1948; see also Ambartsumyan 1958). Furthermore, radiation that is emitted in the chromosphere does not always come directly out; it is in many cases, in particular in all the strong resonance lines, scattered many times before emerging. And, as a consequence of this line scattering together with continuous absorption, there is some radiative transfer of energy within the chromosphere, particularly in the lower levels. Thus the observations cannot be directly used to find the rate of heating at each height in the chromosphere, and in the absence of the complete solution of the transfer problem we can use the measured data only to estimate the dissipation in the entire chromosphere and in the corona. The observations may also be supplemented by theoretical calculations of the energy emitted by various processes important in the different layers.

Apparently, the most important single mechanism of energy loss is the H^- continuum emitted by the lowest levels of the chromosphere. According to Minnaert (1953), the optical depth in the continuum at the visible limb of the sun, $h = 0$, is $\tau = 0.003$, while, according to van de Hulst (1953), the temperature increases outward beginning at this same height. If δT is the mean temperature excess of this layer over the temperature it would have in the absence of non-radiative heating, namely, T_0, the boundary temperature of the sun, then the excess outward flux πF_+ in the continuum is approximately given by

$$\pi F_+(\mathrm{H}^-) = 4\sigma T_0^3 \delta T \tau , \tag{1}$$

and with $T_0 = 4600°$, $\delta T = 200°$, $\tau = 0.003$, the result is $\pi F_+(\mathrm{H}^-) = 1.5 \times 10^7$ ergs/cm^2 sec. The uncertainty is large, because the values of T_0 and δT are known only approximately.

In the Lyman continuum of atomic H, the chromosphere is optically thick, and the NRL rocket observational results quoted by Morton and Widing (1960*a*) give $T = 6900°$ K for the equivalent black-body temperature just short of the Lyman limit, corresponding to an outward flux of only $\pi F_+(\text{Ly C}) = 3 \times 10^2$ ergs/cm² sec. However, in the other continua of H the chromosphere is optically thin, and the energy radiated can be calculated from the emission coefficients. The necessary formulae have been given in convenient form by Parker (1953) and Cillié (1932), and j, the emission coefficient per unit volume (integrated over all solid angles), can be written

$$j(\text{Ba, Pa, . . . , C}) = 8.94 \times 10^{-23} \frac{N_i N_e}{T^{1/2}}, \tag{2}$$

where (Ba, Pa, . . . , C) is intended to represent the Balmer, Paschen, and all other higher continua of H. The flux emitted in the outward direction in these continua, then, is

$$\pi F_+(\text{Ba, Pa, . . . , C}) = \tfrac{1}{2} \int j\, dh \tag{3}$$

where h is the height co-ordinate, and for the chromospheric model tabulated by van de Hulst (1953), the result is $\pi F_+(\text{Ba, Pa, . . . , C}) = 5 \times 10^5$ ergs/cm² sec. The free-free contribution is even smaller than the bound-free emission at chromospheric temperatures, and thus we conclude that the main energy loss in the continuum is due to H^-.

The flash spectrum in the visible region is dominated by hydrogen lines, and we must therefore also estimate their importance in cooling the chromosphere; this calculation is quite difficult to make, and the results are highly uncertain. The higher Balmer lines in the flash spectrum are not affected by self-absorption, so the distribution with height of the emitting atoms can be calculated from the eclipse observations, and then the flux emitted in the outward direction can be found (see, e.g., Menzel and Cillié 1935). In this way we obtain from the results for the 1952 eclipse given by Athay, Billings, Evans, and Roberts (1954) corrected by Athay, Menzel, and Orrall (1957) the flux emitted in all the higher Balmer lines ($10 \leq n < \infty$) to be $\pi F_+ = 2 \times 10^6$ ergs/cm² sec.

The lower Balmer lines in the flash spectrum are affected by self-absorption, and the computation of the outward flux therefore involves more assumptions. For instance, according to Woltjer (1954), the intensity in Hα in the direction tangent to the sun's limb at the base of the chromosphere is about $I = 3.5 \times 10^5$ ergs/cm² sec sterad. The observations show definitely that the chromosphere is optically very thick at the center of this line in this direction, and, if it were equally optically thick in all directions, then the outward flux in Hα would simply be $\pi F_+ = \pi I = 1 \times 10^6$ ergs/cm² sec. However, also according to Woltjer (1954), the Hα line arises completely in the spicules, which are idealized as long thin columns directed radially to the solar surface and covering in projection only 2 per cent of it. According to this model, the outward flux is only 4 per cent (because of projection effects) of the value above, that is, about 4×10^4 ergs/cm² sec. Finally, according to De Jager (1957*a*), the optical depth at the center of Hα of the interspicular matter is about 0.15, so its contribution to the outward Hα flux may be as large as 1.5×10^5 ergs/cm² sec, and, furthermore, the spectroheliograms show that much more than 2 per cent of the solar disk is bright, presumably because there are many more emitting regions low in the chromosphere that are not observed as spicules at the limb. Thus the outward flux in Hα from the chromosphere is decidedly uncertain; but we will estimate it as about 5×10^5 ergs/cm² sec. The other lower Balmer lines Hβ, Hγ, . . . , H9 presumably have fluxes intermediate between the fluxes in Hα and in the higher lines, and our final estimate for all the Balmer lines together, Hα through H∞, is $\pi F_+ = 4 \times 10^6$ ergs/cm² sec.

Among the strongest lines in the flash spectrum are the H and K lines of Ca II, and their flux can be found from direct observations of the disk. The equivalent width of the K_2 emission feature in the case of the K line, as seen in quiet regions at the center of the

disk, is about 0.002 A (Goldberg, Mohler, and Muller 1959), corresponding to a flux of only about 1.2×10^4 ergs/cm² sec. Stronger resonance lines of other metals, however, occur farther in the ultraviolet and must also be taken into account. This spectral region has been very completely discussed by De Jager (1955), but many new observational results have since become available. Among the strongest ultraviolet lines that arise in the chromosphere are the Si II pair λ 1808, λ 1816, with a measured outward flux about 1.3×10^5 ergs/cm² sec (Aboud, Behring, and Rense 1959), and the Mg II pair λ 2791, λ 2798, with a measured flux of the order of 2.5×10^5 ergs/cm² sec (Clearman 1953; Johnson, Purcell, Tousey, and Wilson 1953). The fluxes due to all the metallic lines together thus probably add up to a few times 10^6 ergs/cm² sec and are not as important as the H^- continuum but are perhaps almost comparable with the Balmer line emission.

Thus our final result is that the part of the radiative flux of energy outward from the chromosphere that is balanced by non-radiative heating processes can best be estimated as about 2×10^7 ergs/cm² sec, but this estimate is highly uncertain and could easily be reduced or increased by a large factor, of the order of 3 or so. Since there must be an equal flux directed inward from the chromosphere toward the photosphere, the best estimate of the total non-radiative energy supplied to the chromosphere is about 4×10^7 ergs/cm² sec.

These estimates are all intended to apply to the quiet, undisturbed sun. It is known that in the plages, which appear bright on Ca II spectroheliograms, the magnetic field is large (Babcock and Babcock 1958; Howard 1959; Leighton 1959) and the chromospheric and coronal emissions are both enhanced (Athay and Thomas 1957). About the only available quantitative data for the chromosphere is that the flux in the Ca II K line from a plage is often five times as high as from the undisturbed sun, that is, it can be 7×10^4 ergs/cm² sec or even more (Smith 1960). Either the strengthening of this single line could represent an increased flux of energy into the plage region, or else the dissipation in more favorable circumstances for producing the K line of the same flux of energy as is available in the undisturbed chromosphere. The fact that the entire chromospheric spectrum is strengthened, particularly the lines formed at high temperatures (Athay and Thomas 1957), favors the first alternative, but the additional flux is not known quantitatively.

The outward radiative flux for the corona, which must be completely balanced by non-radiative heating, has been estimated by Woolley and Allen (1948) as about 9×10^3 ergs/cm² sec, the greatest part in the Mg X λ 610 emission line. The far ultraviolet and X-ray rocket observations of the sun have been summarized by Friedman (1959, 1960), and they show that there is considerable emission, presumably almost entirely from the corona, in the wave-length interval 10–200 A. The best estimate for the outward flux in this region from the quiet sun near sunspot minimum is about 6×10^3 ergs/cm² sec, and the Mg X line, though it is observed, is probably somewhat weaker than the calculated value above. Making some allowance for the longer-wave-length emission and doubling the outward flux to account for the inward radiation also, we estimate the total radiative heat flux from the quiet corona to be around 1.5×10^4 ergs/cm² sec, with again a large uncertainty because it is a value based on a relatively few observations.

The rocket observations also show that the X-ray emission from the corona can be eight times as high as the value given above, at times around sunspot maximum, when the coronal excitation as measured by the relative strength of (Fe XIV) 5303 is also a maximum (Friedman 1960). Thus the energy flux into the corona is considerably larger at these times (none of the observations used in this discussion were made at times of flares, which can enhance the solar X-ray emission even more).

Finally, we discuss the observed flux in the Lyman-α line, for which the measurements made with ion chambers since October, 1955, all give about 3×10^5 ergs/cm² sec (Friedman 1960). Earlier measurements with other instruments had suggested smaller and variable fluxes, but they are perhaps less reliable, and, since for the period October, 1955, through March, 1958, covering the sunspot cycle from just after minimum to maximum,

all the measurements give essentially the same flux, there is no strong observational evidence for variation. However, the Lyman-α radiation comes almost entirely from plage regions (Purcell, Packer, and Tousey 1960), and, since these vary greatly in size and number through the sunspot cycle, it seems likely that there should be some changes in the flux. Now it appears both on theoretical grounds (Woolley and Allen 1950) and from the interpretation of the observed Lyman-α profile (Morton and Widing 1960*a*, *b*) that the line arises in the transition region between the chromosphere and corona and, furthermore, that it is likely that this region is heated by conduction of heat inward from the corona (Giovanelli 1949; Woolley and Allen 1950). Therefore, the energy radiated by the sun in the Lyman-α line is balanced ultimately by non-radiative energy dissipated mostly in the corona, and this must be taken into account in calculating the energy balance. The other lines possibly of importance in the transition layer, such as the He II resonance line λ 304, higher Lyman lines, and lines of intermediate ionization in the far ultraviolet, are all considerably weaker than Lyman-α (Friedman 1960; Hinteregger, Damon, Heroux, and Hall 1960). Because of the observed variation of the coronal X-ray fluxes and because the Lyman-α situation is still somewhat in doubt, it has been assumed here that there is some variation in the Lyman-α flux with the sunspot cycle and that the outward flux 3×10^5 ergs/cm^2 sec refers to sunspot maximum, while we will more or less arbitrarily assume 1×10^5 ergs/cm^2 sec as the outward flux from the undisturbed sun at sunspot minimum. These figures probably do not have to be doubled, because the Lyman-α photons emitted in the inward direction most likely are scattered back out without absorption, but this is not certain. This is the best estimate we can make of the energy loss by the corona, though it would be too high if it turned out that a large fraction of the Lyman-α radiation originated in the lower chromosphere and was scattered without absorption until it diffused out; in this case the energy loss by the corona could not be less than 1.5×10^4 ergs/cm^2 sec derived above from the X-ray data.

All these figures are in fair, though by no means perfect, agreement with the set of results presented by De Jager (1959), who gives 3×10^4 ergs/cm^2 sec for the energy loss by radiation of the corona and 2.5×10^5 ergs/cm^2 sec for the energy loss of the transition layer, together with an independent estimate, based on radio determinations of the temperature gradient, of the energy conducted back from the corona to the transition layer as 4×10^5 ergs/cm^2 sec.

The measurements of the large-scale solar magnetic fields have been summarized by Babcock and Babcock (1958). They show that, in high latitudes, fields of the order of 1 gauss often cover large areas, while, in addition, at lower latitudes large UM and BM regions, often centered on sunspots but covering a much greater area than the plages, have aligned fields of the order of 1 to several gauss. Both types of fields are, very approximately, directed mostly radially to the sun's surface, and, though all published measures have been made with absorption lines formed in the photosphere, nearly the same fields must extend up into the chromosphere and lower corona. In the present paper 2 gauss and occasionally 0.5 gauss have been adopted as representative values for the magnetic fields of the sun outside plage regions.

In the plages, however, the fields are considerably larger. Detailed measurements with high angular resolution made by Howard (1959) and Leighton (1959) show that wherever the field is larger than about 20 gauss, a plage can be distinguished on a calcium spectroheliogram, while fields as high as 100 gauss are observed in these plages (but outside the spots, where the fields are even higher). We have adopted 50 gauss as a representative value of the field in a plage.

III. MAGNETOHYDRODYNAMIC WAVES

In a compressible gas, small disturbances propagate as sound waves, at the velocity of sound V_S given by

$$V_S = \sqrt{\frac{\gamma P}{\rho}}, \tag{4}$$

and the motion of the material is longitudinal, that is, in the direction of propagation. On the other hand, in an incompressible fluid that is a good electrical conductor and is in a magnetic field, small disturbances propagate in the direction of the field as magnetohydrodynamic or Alfvén waves, at the Alfvén velocity, V_A, given by

$$V_A = \frac{B}{\sqrt{(4\pi\rho)}}, \tag{5}$$

and the motion is transverse to the direction of propagation. In an electrically conducting compressible gas in a magnetic field, mixed forms of the waves occur, and they have been analyzed by Herlofson (1950) and van de Hulst (1951), as well as by several later authors, in most detail by workers at New York University (Bazer and Ericson 1959; Bazer and Fleischman 1959; Grad 1959) and, very recently, by Lighthill (1960). The properties of the various types of modes are described in the listed references, but we summarize here very briefly the main features that are important for our problem.

In general, there are three types of waves—the fast mode, slow mode, and Alfvén mode. The fast mode can propagate in any direction, and the phase velocity V_F is given by

$$V_F^2 = \tfrac{1}{2}\{V_S^2 + V_A^2 + [(V_S^2 + V_A^2)^2 - 4V_S^2 V_A^2 \cos^2\theta]^{1/2}\}, \tag{6}$$

where θ is the angle between the direction of the magnetic field and the normal to the wave front. For a very weak magnetic field, $V_S \gg V_A$ and $V_F = V_S$, while, for a very strong field, $V_S \ll V_A$ and $V_F = V_A$; in both these limiting cases the velocity is independent of the direction of propagation, while at intermediate fields the velocity depends weakly on the direction. The most extreme variation occurs when $V_S = V_A = V$, in which case

$$V_F^2 = V^2[1 + \sin\theta]. \tag{7}$$

At weak fields the direction of material motion is longitudinal, and the waves are essentially sound waves, while at large fields the motion is perpendicular to the direction of the field and lies in the plane of propagation, and the waves are essentially magnetohydrodynamic in character. Numerical values of the velocity of sound and of Alfvén waves are given in Table 2, derived from the models given for the photosphere by Minnaert (1953) and the chromosphere and corona by van de Hulst (1953). It can be seen that, for all reasonable assumed field strengths, the fast-mode disturbances are sound waves in the hydrogen convection zone and photosphere, and magnetohydrodynamic waves in the upper chromosphere and corona, the transition occurring in the lower chromosphere. (Since there is some question whether the sound waves propagate nearly adiabatically, with $\gamma = 1.67$, or more nearly isothermally, with $\gamma = 1.00$, a harmonic mean $\gamma = 1.29$ has been assumed in all the calculations of the present paper, going over smoothly at depths below -200 km to the adiabatic value $\gamma = 1.67$ at -400 km.)

The slow mode can propagate only in directions close to the direction of the magnetic field, and both at very weak fields, $V_S \gg V_A$, and very strong fields, $V_S \ll V_A$, the only allowed direction of propagation is exactly along the field, while at an intermediate field, $V_S = V_A$, the allowed directions lie within a cone with half-angle $\chi = \tan^{-1} 0.5 = 27°$. The velocity of these slow-mode disturbances, along the direction of the field, is approximately V_A for $V_S > V_A$, and V_S for $V_S < V_A$. The material motion is perpendicular to the direction of propagation and in the plane containing the magnetic field for $V_S \gg V_A$ and is in the direction of the field for $V_S \ll V_A$.

Finally, the Alfvén mode in the compressible case has the same properties as in an incompressible fluid; it propagates in the direction of the magnetic field with the Alfvén velocity V_A, and no change in density or pressure is involved.

Some laboratory experiments have been performed to verify the predicted properties

of magnetohydrodynamic waves in a conducting liquid, but the observations of disturbances propagating through the earth's ionosphere are most relevant to the astronomical case of a compressible gas. Such shock disturbances have been detected traveling up through the ionosphere as a result of atomic-bomb explosions on the ground (Daniels, Bauer, and Harris 1960), and also the effects resulting from disturbances generated by high-altitude bomb tests have been measured on the ground (Berthold, Harris, and Hope 1960). In both cases two separate disturbances arrived at the point of detection, with time delays which could be identified with the Alfvén and sound velocities, and, since in the ionosphere $V_S < V_A$, presumably one disturbance was a combination of fast and Alfvén modes, while the other was a slow-mode shock.

TABLE 2

SOUND AND ALFVÉN VELOCITIES IN SOLAR ATMOSPHERE

Height h (km)	Sound Velocity V_S (km/sec)	Alfvén Velocity V_A (km/sec)	
		$B=2$ gauss	$B=50$ gauss
+6000	10 3	57 7	1440
+5000	9 7	41 0	1020
+4000	8 7	25 8	644
+3000	8 0	16 3	407
+2000	7 4	7 3	181
+1500	7 0	2 6	65
+1000	6 7	0 82	20
+ 750	6 6	0 41	10 2
+ 500	6 5	0 20	5 0
+ 250	6 4	0 092	2 3
0	6 3	0 041	1 0
− 100	6 4	0 025	0 62
− 200	6 5	0 015	0 38
− 300	6 7	0 010	0 25
− 350	7 6	.....	..
− 400	8 2	0 0082	0 20
− 450..	9 0		

IV. GENERATION OF WAVES

We now examine in detail the generation of small-amplitude waves by the turbulent motion in the hydrogen convection zone, the original source of the energy for the chromospheric heating mechanism we are considering. Since the fast-mode waves are, as seen in the previous section, sound waves to a very good approximation in the hydrogen convection zone, the problem is the generation of acoustical noise by turbulence. It has been studied quantitatively by Lighthill (1952), and a numerical estimate of the amount of sound produced was made by Proudman (1952), while the theory was further worked out, compared with experiment, and summarized by Lighthill (1954). All these papers deal with isotropic turbulence, while in the sun there is a preferred direction—the radial direction; however, it is apparently a fairly good approximation to treat the turbulence as locally isotropic but with properties that vary in the preferred direction (Lighthill 1954). The rate of generation of acoustic noise per unit volume derived by Lighthill (1952) is

$$j_1 = a\rho\epsilon\left(\frac{\langle v^2\rangle}{V_S^2}\right)^{5/2} = a\rho\frac{(\langle v^2\rangle)^4}{V_S^5 l}, \tag{8}$$

where $(\langle v^2 \rangle)^{1/2}$ is the root mean square of one component of the turbulent velocity, ϵ is the rate of dissipation per unit mass, given in terms of the scale length of turbulence l, by

$$\epsilon = \frac{(\langle v^2 \rangle)^{3/2}}{l}, \tag{9}$$

ρ is the density, and α is a numerical constant which depends only weakly on the form of the spectrum of turbulence and has the value 38 for the Heisenberg spectrum (Proudman 1952). The result is approximately confirmed by experimental measurements of the noise due to turbulence produced by jets of gas escaping into air (Lighthill 1954).

We have applied this formula to the model solar hydrogen convection zone calculated by Vitense (1953) under the assumption $l = H$, that is, that the scale length of the turbulence is identical with the local scale height of the atmosphere. The calculation is summarized in Table 3 (the velocity of sound was assumed to have the adiabatic value at

TABLE 3

ACOUSTICAL ENERGY GENERATED IN HYDROGEN CONVECTION ZONE

h (km)	$\langle v^2 \rangle^{1/2}$ (km/sec)	l (km)	ρ (gm/cm^3)	V_S (km/sec)	j_1 (ergs/cm^3 sec)
−350	0 0	127	$2\ 9\times10^{-7}$	7 6	0 00
−400	0 5	148	3 1	8 2	0 00004
−450	2 3	175	3 3	9 0	9 55
−525	2 1	206	3 6	9 6	2 94
−600	1 8	227	4 0	10 2	0 68
−700	1 5	281	$5\ 2\times10^{-7}$	11 3	0 097

these great depths), where it can be seen that, because of the strong dependence on turbulent velocity, practically all the energy is generated in a narrow shell between 425 and 550 km in depth.

The upward flux of energy in the form of sound waves πF_+, is then calculated by integration through the emitting layers,

$$\pi F_+ = \tfrac{1}{2} \int j_1 dh = 3.3 \times 10^7 \text{ ergs/cm}^2 \text{ sec}, \tag{10}$$

a result in very satisfactory agreement with the estimate (made in Sec. II) of the energy dissipated in the chromosphere. Indeed, the sensitivity of the numerical value of the turbulent velocity, which, of course, is not exactly known, is so high that one can only say that there is no disagreement between the calculations of the energy generated in the hydrogen convection zone and the excess energy radiated by the chromosphere.

The frequency spectrum of the sound waves emitted by turbulence has been discussed from the experimental point of view by Lighthill (1954) and in terms of the spectrum of turbulence by Meecham and Ford (1958). The resulting energy spectrum of noise drops off to zero at high frequencies as $\nu^{-7/2}$ and at very low frequencies as ν^4, while at intermediate frequencies it depends strongly on the spectrum of turbulence, including the large eddies, which depend, in turn, on the energy-input mechanism and thus are not described by the universal Heisenberg spectrum. The experiments in air generally show that the spectrum is relatively broad, with a flat peak at a frequency near

$$\nu_0 = \frac{(\langle v^2 \rangle)^{1/2}}{l}, \tag{11}$$

dropping off at lower frequencies until the intensity is down by a factor of 100 at a frequency of about 0.1 ν_0. At higher frequencies the intensity drops off rapidly above a frequency ν_1, at which the acoustical wave length is equal to the scale length of turbulence,

$$\nu_1 = \frac{V_S}{l} = \frac{V_S}{\langle v^2 \rangle^{1/2}} \nu_0 , \tag{12}$$

because, for these short wave lengths, interference effects within a turbulent eddy reduce the emitted sound (Lighthill 1954).

If there is a large mean shear, that is, a flow in which

$$\frac{dV_x}{dy} > \frac{\langle v^2 \rangle^{1/2}}{l} , \tag{13}$$

then additional noise is generated by the shear flow, mostly at frequencies above ν_1. In the hydrogen convection zone, however, we generally think of the motions as nearly completely turbulent, and this source of noise can then be disregarded.

Thus we shall consider the spectrum of fast-mode disturbances to be relatively flat, with a maximum at the frequency

$$\nu_0 = \frac{\langle v^2 \rangle^{1/2}}{l} = 1.2 \times 10^{-2} \text{ sec}^{-1} , \tag{14}$$

and with nearly all the power included between the frequencies

$$\begin{aligned} \nu_{\min} &= \tfrac{1}{4}\nu_0 , \\ \nu_{\max} &= \nu_1 = 4\nu_0 , \end{aligned} \tag{15}$$

where all the numerical values are estimated for a mean level near the center of the noise-producing region.

Next we must discuss the effects of magnetic fields on the generation of fast-mode disturbance, and this requires some knowledge of the magnetic field within the hydrogen convection zone. This field is not directly observed, because the absorption lines used in the solar magnetograph measurements (Babcock and Babcock 1955, 1958) are all formed higher up in the photosphere. However, the difference in depth is so small that there is no doubt that the mean organized field hardly changes at all from the photosphere to the noise-producing layer. But it is not so clear whether or not there is a much larger turbulent magnetic field within the hydrogen convection zone; there are arguments for and against the idea of equipartition between turbulent kinetic and magnetic energies, which have been summarized by Cowling (1953, 1957). In the present paper we have adopted the picture that over most of the area of the sun the magnetic field in the hydrogen convection zone is small but that, in the plage regions where the surface field is of the order of 50 gauss, the turbulent field in the hydrogen convection zone has the equipartition value

$$\langle b^2 \rangle^{1/2} = (4\pi\rho \langle v^2 \rangle)^{1/2} = 450 \text{ gauss} \tag{16}$$

for the root mean square of one component. It is hard to see how the plages can preserve their existence for periods of days or weeks without having a fairly large field below them, and, in addition, as will be seen in the succeeding sections, it seems to be the only way in which the enhanced chromospheric and coronal emission in excited regions can be understood.

The generation of magnetohydrodynamic waves by isotropic turbulence has been investigated by Kulsrud (1955), who again found that the results were not extremely sensi-

tive to the adopted form of the spectrum. The presence of an equipartition turbulent magnetic field increases the rate of energy generation in the fast-mode disturbances by a factor 10, while the presence of a constant field much smaller than the equipartition value does not essentially affect the result at all. Furthermore, essentially no energy is delivered into the Alfvén or slow modes as long as the constant field is considerably below the equipartition value, though this result is an estimate not based on calculation. Thus, no matter what the constant magnetic field is (so long as it is smaller than several hundred gauss), energy is generated only in the fast-mode waves, and the upward flux at the bottom of the photosphere varies from about 3×10^7 ergs/cm^2 sec in the undisturbed sun to about 3×10^8 ergs/cm^2 sec in the plage areas.

The work of Kulsrud (1955) is based on the calculation of the quadrupole emission of sound by the fluctuating turbulent velocity and magnetic fields. However, in the case of a finite constant magnetic field, additional dipole terms may, in general, be expected to enter the expression for the emission. Our next problem is therefore to estimate approximately their magnitude. Following the method and notation of Kulsrud (1955), the equation for sound propagation is found to be

$$\frac{\partial^2 \rho}{\partial t^2} - a_0^2 \frac{\partial^2 \rho}{\partial x_j \partial x_j} = \frac{\partial^2 (\rho v_i v_j)}{\partial x_i \partial x_j} - \frac{1}{4\pi} \frac{\partial}{\partial x_j} \{ (\nabla \times \boldsymbol{b}) \times (\boldsymbol{B} \times \boldsymbol{b}) \}_j . \tag{17}$$

The excess sound energy emitted as a consequence of the constant magnetic field $\boldsymbol{B}$ has the second term on the right-hand side as a source, and, if we write

$$\boldsymbol{F} = (\nabla \times \boldsymbol{b}) \times \boldsymbol{B} , \tag{18}$$

we find, following the arguments and notation used by Lighthill (1952), the intensity of sound resulting from it to be

$$I(\boldsymbol{x}) = \frac{1}{16\pi^2 \rho_0 a_0^3} \int\int \frac{x_i x_j}{x^4} \frac{\partial}{\partial t} F_i \left(\boldsymbol{y}, t - \frac{|\boldsymbol{x} - \boldsymbol{y}|}{a_0} \right) \frac{\partial}{\partial t} F_j \left(\boldsymbol{z}, t - \frac{|\boldsymbol{x} - \boldsymbol{z}|}{a_0} \right) d\boldsymbol{y}\, d\boldsymbol{z} \tag{19}$$

at great distances $\boldsymbol{x}$ from the source. Finally, the total acoustical energy output integrated over all directions from this source may be written

$$\int j_2 d z = \frac{1}{12\pi \rho a_0^3} \int\int \frac{\partial}{\partial t} F_i \left(\boldsymbol{y}, t - \frac{|\boldsymbol{x} - \boldsymbol{y}|}{a_0} \right) \frac{\partial}{\partial t} F_i \left(\boldsymbol{z}, t - \frac{|\boldsymbol{x} - \boldsymbol{z}|}{a_0} \right) d\boldsymbol{y}\, d\boldsymbol{z} . \tag{20}$$

Now, for the constant field $\boldsymbol{B} = B_0 \boldsymbol{k}$ in the z-direction,

$$F_x = \frac{B_0}{4\pi} \frac{\partial b_x}{\partial z}, \qquad F_y = \frac{B_0}{4\pi} \frac{\partial b_y}{\partial z}, \qquad F_z = 0 , \tag{21}$$

and the dipole emission per unit volume may finally be approximately estimated to be

$$\begin{aligned} j_2 &= \beta \frac{1}{\rho V_S^3} \left(\frac{B_0}{4\pi} \right)^2 \frac{\langle b^2 \rangle}{t^2 l^2} l^3 \\ &= \beta \frac{B_0^2 \langle b^2 \rangle \langle v^2 \rangle}{16\pi^2 \rho V_S^3 l} , \end{aligned} \tag{22}$$

where β is a numerical constant, in principle to be evaluated from an integration over the turbulent spectrum, analogous to α in equation (8); l, as before, is a characteristic length of the turbulence; t a characteristic time, defined by

$$t = \frac{l}{\langle v^2 \rangle} ; \tag{23}$$

$\langle b^2 \rangle$ is the root-mean-square component of the turbulent magnetic field; and we have again labeled the velocity of sound V_S, instead of a_0, as in equations (17)–(20). Then, if we adopt the equipartition turbulent magnetic field of equation (16), the sound-wave generation by this process is given by the emission coefficient

$$j_2 = \beta \frac{B_0^2}{4\pi} \frac{\langle v^2 \rangle^2}{V_S^3 l}. \tag{24}$$

Comparing this expression with equation (8), which gives the quadrupole emission in the absence of a field, we have

$$\frac{j_1}{j_2} = \left(\frac{\alpha}{\beta}\right)\left(\frac{4\pi\rho\langle v^2 \rangle}{B_0^2}\right)\left(\frac{\langle v^2 \rangle}{V_S^2}\right), \tag{25}$$

and, for the energy-producing region in the solar hydrogen convection zone, the second and third factors approximately cancel for $B_0 = 120$ gauss. Since β has not been evaluated, we can only use an estimate of its value, and, under the plausible assumption that α and β are approximately the same, it follows that the dipole process never adds significantly to the fast-mode emission, because for small fields $j_1 \gg j_2$, while for the largest plage fields $j_1 \approx j_2$ but the wave generation due to the turbulent magnetic-field quadrupole process is, as stated above, then about $10 j_1$. If, on the other hand, $\alpha/\beta = 0.1$, the dipole effect would double the fast-mode emission at the largest plage fields.

Here we have seen that the introduction of a constant magnetic field removes the isotropy and causes dipole terms to enter the wave-emission coefficient. Cowling has suggested that, even in the absence of a magnetic field, the pressure and density gradients define a preferred direction, and there might be additional dipole emission of sound waves due to them; but we have not yet investigated this question.

V. PROPAGATION OF FAST-MODE DISTURBANCES

We shall describe the propagation of wave energy through the photosphere and chromosphere by calculating the rays followed by waves originating in the hydrogen convection zone, in a way exactly analogous to geometrical optics. Since the wave lengths are typically of the order of 700 km, while the depth of the wave-emitting zone is only about 450 km below the surface and the whole height traveled by the waves only a few thousand kilometers, this cannot be expected to be a very precise scheme, but it should give the general features of the way in which the energy is transported. The alternative—to integrate the relevant differential equations—is mathematically quite complicated even for the case of a steady state (standing waves) in an atmosphere with constant scale height and with no allowance for dissipation (Ferraro and Plumpton 1958; Weymann and Howard 1958) and has not yet been worked out for the case of a damped traveling wave. The ray treatment of material waves was applied to the chromosphere by Schatzman (1949), and it has been particularly exploited for pure gas-dynamic shocks by Keller (1954) and for magnetohydrodynamic disturbances by Bazer and Fleischman (1959).

First, we discuss the angular dependence of the intensity of the sound waves near the layer in which they are generated in the hydrogen convection zone. Since this layer is quite thin, if we neglect refraction, absorption, and scattering altogether, we can simply derive the intensity of sound energy emerging at a particular angle ϕ from the vertical:

$$I(\phi) = \frac{1}{4\pi} \int j_1 ds = \frac{1}{4\pi \cos\phi} \int j_1 dh = \frac{I_0}{\cos\phi}, \tag{26}$$

and the total flux in the upward direction,

$$\pi F_+ = 2\pi \int_0^{\pi/2} I(\phi) \cos\phi \sin\phi d\phi \qquad (27)$$
$$= 2\pi I_0 = \tfrac{1}{2} \int j_1 dh ,$$

where s is the co-ordinate along the ray, h is the height, and the integrals are taken through the entire emitting layer. According to equation (26), the intensity diverges at $\phi \rightarrow \pi/2$, and this actually would be correct for a horizontally infinite layer without absorption, but in the sun the flux is limited by at least two separate effects. One is that, on account of the curvature of the sun's surface, the path length of a ray through a layer of vertical extent h_0 reaches a finite limit given by

$$y = \sqrt{(2 h_0 R)} \qquad (28)$$

as the angle to the vertical tends to $\pi/2$ from below, where R is the sun's radius. As a result, the intensity reaches an upper limit approximately given by

$$I = I_0 \sqrt{\left(\frac{2R}{h_0}\right)}; \qquad (29)$$

and, in the case of the sun, with $h_0 = 80$ km about, $R = 7 \times 10^5$ km, the upper limit to the path length is about $y = 10^4$ km, corresponding to an upper limit to I of about $10^2 I_0$.

A second cause for a finite intensity even in the horizontal direction is the scattering of sound by turbulent eddies within the hydrogen convection zone. We can estimate this effect approximately by analogy to the optical case, assigning to an eddy in which the velocity of sound differs from the mean velocity V_S by an amount δV_S an index of refraction n, given by

$$n - 1 = -\frac{\delta V_S}{V_S}. \qquad (30)$$

In the optical theory, the scattering cross-section depends on the parameter

$$x = \frac{\pi D}{\lambda} = \frac{\pi l}{\lambda} = \frac{\pi V_S}{\langle v^2 \rangle^{1/2}} = 0.8 , \qquad (31)$$

where we have taken the mean eddy diameter D to be the same as the turbulent scale length l, and the numerical value is computed for the region of greatest contribution to the emission coefficient. For this value of x, the scattering cross-section is given by the Rayleigh-Gans theory as

$$Q = 0.4 \left(\frac{\delta V_S}{V_S}\right)^2 \pi l^2 \qquad (32)$$

(van de Hulst 1957), and it only remains to estimate $(\delta V_S / V_S)$. It appears that fluctuations in the sound velocity in the hydrogen convection zone are minor in comparison with convective effects, that is, that an eddy moving with speed v carries the sound along with it and gives it a speed, in a stationary reference system, of $V_S + v$, so we may identify $\delta V_S = \langle v^2 \rangle^{1/2}$, the mean turbulent velocity, and thus find $Q = (\pi/40) l^2$; that is, a sound wave penetrates about 40 eddies or a distance of 7×10^3 km before being strongly scattered. This calculation is quite schematic, but it is correct in order of magnitude, and we see that each of the two effects discussed sets an upper limit of about $10^2 I_0$ to the intensity of sound in the nearly horizontal directions in the hydrogen convection zone.

In discussing the upward propagation of the waves, we must take some account of the reflection of sound energy by the density gradient (Biermann 1948). The scale height H

in the photospheric layers is roughly constant (see Table 4), and so the theory of sound waves in an atmosphere with constant scale height (see Lamb 1945) may be used as a guide. According to this theory, there is a critical frequency,

$$\nu_c = \frac{V_S}{4\pi H}, \tag{33}$$

and waves with frequencies equal to or higher than this frequency are transmitted undamped (though waves with frequencies just above the critical frequency suffer a dispersion in velocities), while waves with frequencies below the critical frequency are reflected, with the energy transported by the waves decreasing by a factor e in a distance

$$h_1 = \frac{H}{[1 - (\nu/\nu_c)^2]^{1/2}}. \tag{34}$$

TABLE 4

SCALE HEIGHT AS FUNCTION OF HEIGHT IN SOLAR ATMOSPHERE

Height h (km)	Scale Height H (km)	Height h (km)	Scale Height H (km)
−350	223	100	140
−300	148	250	170
−200	113	500	180
−100	101	1000	200
0	85		

Thus only sound with frequency above the critical frequency for a layer with just about the minimum scale height, say $H = 100$ km, penetrates through the photosphere and reaches the chromosphere above $h = 1000$ km; and, since

$$\nu_c = \frac{7 \text{ km/sec}}{4\pi \times 100 \text{ km}} = 6 \times 10^{-3} \text{ sec}^{-1}, \tag{35}$$

so that $\nu_{\min} < \nu_c < \nu_0$, nearly but not quite all the spectrum of acoustical noise produced in the hydrogen convection zone penetrates to the chromosphere.

Now we shall examine the effects of refraction in the transport of wave energy up into the chromosphere. In general, the fast-mode velocity V_F depends on direction, though in the limits $V_S \gg V_A$ and $V_S \ll V_A$ it does not, and the maximum difference between horizontal and vertical velocities is only 40 per cent at $V_A = V_S$ (see Sec. III). Though it is possible to find the ray paths taking this directional dependence into account (Bazer and Fleischman 1959), the calculations are unduly complicated for a preliminary study, and we have therefore simplified the problem by taking the velocity to be independent of direction, and to have the values

$$\begin{aligned} V_F^2 &= V_S^2 + \tfrac{1}{2} V_A^2 \quad \text{for} \quad V_S > V_A, \\ V_F^2 &= V_A^2 + \tfrac{1}{2} V_S^2 \quad \text{for} \quad V_S < V_A, \end{aligned} \tag{36}$$

as an approximate average from equation (6). Velocities calculated according to these formulae for fields of $B = 0.5$ and 2 gauss, representing the undisturbed sun, and $B = 50$

gauss, representing a plage area, are given in Table 5, derived from the data of Table 2.

The ray paths may then be calculated directly according to the methods of geometrical optics, from the equation

$$n \sin \phi = \text{const.}, \tag{37}$$

where n is the relative index of refraction, given by

$$n = \frac{V_0}{V_F}, \tag{38}$$

TABLE 5

FAST-MODE VELOCITIES IN SOLAR ATMOSPHERE

HEIGHT h (km)	FAST-MODE VELOCITY V_F (km/sec)		HEIGHT h (km)	FAST-MODE VELOCITY V_F (km/sec)	
	$B=2$ gauss	$B=50$ gauss		$B=2$ gauss	$B=50$ gauss
+6000	58 1	1440	+250	6 4	6 6
+5000	41 5	1020	0	6 3	6 3
+4000	26 4	644	−100	6 4	6 4
+3000	17 3	407	−200	6 5	6 5
+2000	9 0	181	−300	6 7	6 7
+1500	7 2	64	−350	7 6	7 6
+1000	6 8	21	−400	8 2	8 2
+750	6 6	11 3	−450	9 0	9 0
+500	6 5	7 4			

V_0 being the velocity at the level where the waves are emitted, $V_0 = 9.0$ km/sec in our case. The maximum height to which a ray with initial direction ϕ_0 penetrates can thus be found immediately by solving

$$\sin \phi_0 = n = \frac{V_0}{V_F}, \tag{39}$$

while the whole ray path can be determined by integrating numerically the differential equation

$$\frac{1}{\sin \phi} = \left[1 + \left(\frac{dh}{dx}\right)^2\right]^{1/2} = \frac{n}{\sin \phi_0} = \frac{V_0}{V_F \sin \phi_0}. \tag{40}$$

Ray paths calculated in this way for $B = 2$ and 50 gauss are shown in Figure 1, where it can be seen that in all cases the rays are first refracted toward the normal because of the decrease of sound velocity outward in the photosphere, then at greater heights are refracted away from the normal because of the increase of Alfvén velocity outward. In all cases the horizontal and vertical distances from the point of emission in the hydrogen convection zone to the turning point in the chromosphere are of the same general order of magnitude.

Finally, we may notice that, because of the increase in sound velocity inward in the hydrogen convection zone, rays emitted in a downward direction (with $\phi_0 > 90°$) do not penetrate very deeply but are refracted back up toward the surface, arriving back at the level from which they were originally emitted with an angle $\phi = 180° - \phi_0$ to the verti-

cal and propagating up into the chromosphere. Thus the entire amount of wave energy generated in the convection zone, not just half of it, is available for dissipation in the chromosphere and corona.

VI. JOULE AND FRICTIONAL HEATING

As magnetohydrodynamic waves propagate through an ionized gas, they dissipate energy by Joule heating at a rate that depends on the electrical conductivity (van de

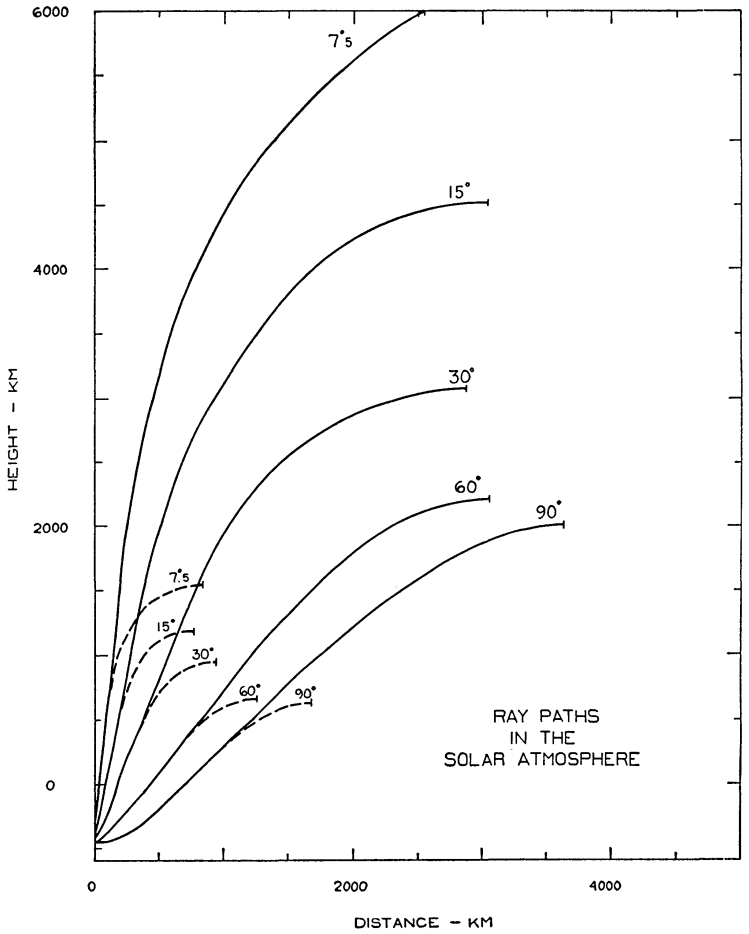

FIG. 1.—Computed ray paths for fast-mode waves in the upper hydrogen convection zone, photosphere, and chromosphere. All rays originate at $h = -450$ km and are labeled with their initial direction to the vertical. *Solid lines*, $B = 2$ gauss; *dashed lines*, $B = 50$ gauss.

Hulst 1953), which in turn depends on the rate of collisions of electrons with positive ions and neutral atoms. Another dissipative process, considerably more effective under many conditions, is the frictional damping due to collisions between the positive ions, which are directly affected by the magnetic-field oscillations, and the neutral atoms, which tend to lag behind (Piddington 1956, 1958). These dissipative effects occur for small-amplitude waves as well as for shocks, and in this section their effect in the heating of the chromosphere is calculated.

For pure Alfvén waves propagating in the direction of the magnetic field in a homoge-

neous medium, ζ_1, the damping length due to conductivity and viscosity (the distance in which the energy flux drops by a factor $1/e$) is given by

$$\zeta_1 = \frac{V_A^3}{4\pi^2\nu^2\,[(c^2/4\pi\sigma) + (\mu/\rho)]} \tag{41}$$

(van de Hulst 1951; Dungey 1958), where σ is the electrical conductivity (in e.m.u. units, sec^{-1}), μ is the viscosity, and c is the velocity of light. The damping length, ζ_2, due to the frictional process is given by

$$\zeta_2 = \frac{V_A}{4\pi^2\nu^2}\,\frac{1+\eta}{\eta\,\tau_n} \tag{42}$$

(Piddington 1956), where η is the ratio of the mass density of neutral atoms to the mass density of ions, while τ_n is the mean collision time of an atom to lose its momentum in

TABLE 6

ALFVÉN-WAVE JOULE-HEATING DAMPING LENGTH

h (km)	log N_e (cm^{-3})	log N_H (cm^{-3})	$c^2/4\pi\sigma$ (cm^2/sec)	μ/ρ (cm^2/sec)	ζ_1 (km)	
					$B=2$ gauss	$B=50$ gauss
− 400	14 8	17 2	$1\ 3\times10^{7}$	$1\ 3\times10^{3}$	$7\ 4\times10^{-2}$	$1\ 2\times10^{3}$
− 300	13 5	17 0	$1\ 4\times10^{8}$	$1\ 6\times10^{3}$	$1\ 4\times10^{-2}$	$2\ 2\times10^{2}$
− 200	12 9	16 7	$2\ 2\times10^{8}$	$3\ 1\times10^{3}$	$2\ 7\times10^{-2}$	$4\ 2\times10^{2}$
− 100	12 5	16 2	2.4×10^{8}	$8\ 3\times10^{3}$	$1\ 1\times10^{-1}$	$1\ 8\times10^{3}$
0	12 0	15 7	$2\ 3\times10^{8}$	$2\ 6\times10^{4}$	$5\ 3\times10^{-1}$	$8\ 2\times10^{3}$
+ 250	11 4	15 2	$1\ 8\times10^{8}$	$8\ 9\times10^{4}$	7 6	$1\ 2\times10^{5}$
+ 500	11 0	14 5	$1\ 3\times10^{8}$	$4\ 6\times10^{5}$	$1\ 1\times10^{2}$	$1\ 7\times10^{6}$
+ 750	10 8	13 9	$6\ 2\times10^{7}$	$1\ 8\times10^{6}$	$2\ 1\times10^{3}$	$3\ 3\times10^{7}$
+1000	10 7	13 3	$2\ 9\times10^{7}$	$7\ 6\times10^{6}$	$2\ 6\times10^{4}$	$4\ 0\times10^{8}$
+1500	10 5	12 3	$1\ 5\times10^{7}$	$1\ 5\times10^{7}$:	$1\ \times10^{6}$:	$1\ \times10^{10}$:
+2000	10 4	11 4	$1\ 2\times10^{7}$			
+3000	10 2	10 6	$1\ 2\times10^{7}$			
+4000	10 0	10 0	$1\ 2\times10^{7}$			
+5000	9 8	9 2	$1\ 1\times10^{7}$			
+6000	9 6	8 4	$1\ 1\times10^{7}$			

collisions with ions. The combined effect is given by the sum of the reciprocals; so the net damping length ζ_0 is

$$\frac{1}{\zeta_0} = \frac{1}{\zeta_1} + \frac{1}{\zeta_2}. \tag{43}$$

For the fast-mode waves in the regions of very strong magnetic field $V_S \ll V_A$, the same expressions apply in the direction of propagation, but the transition region where V_S and V_A are similar in order of magnitude is more complicated and will be discussed below, after we have treated the simpler case of Alfvén waves.

The electrical conductivity set by electron collisions with positive ions is given by Spitzer (1956), while the effect of collisions with neutral atoms, which are particularly important in the photosphere, has been computed by Osterbrock (1952). Furthermore, a table of viscosity coefficients by Edmonds (1957), though intended for the hydrogen convection zone, also covers the photosphere and can be extrapolated slightly to apply to the low chromosphere; the coefficients calculated from these sources are listed in Table 6. At

heights above 1000 km in the chromosphere, the density is too low to apply the viscosity table, but, as we shall see below, the frictional damping process is much more effective at these levels. The damping lengths calculated from these values of the conductivity and viscosity using the Alfvén velocities of Table 2, and the average frequency $\nu_0 = 1.2 \times 10^{-2}$ sec^{-1}, are also listed in Table 6.

Next, to compute the frictional damping length, it is necessary to know the cross-sections for collisions between positive ions and neutral atoms. The most important of these processes are $H^+ + H$, and in the upper chromosphere where hydrogen is nearly completely ionized, $H^+ + He$, while in the photosphere $M^+ + H$, where M is an easily ionized metal, also is effective. Since the main part of the motion between two light atoms is due to their thermal motion, unless the wave oscillations are extremely large, we shall estimate all the cross-sections for a relative energy of motion of 0.75 ev, corresponding to the mean thermal energy at $T = 6000°$ K.

First, in the collision $H^+ + H$, the charge-exchange process $H^+ + H \rightarrow H + H^+$, has a large cross-section, and, since in most of the charge-exchange collisions the nuclei preserve very nearly their original directions of motion (Dalgarno and Yadav 1953), they have the effect of exactly interchanging the directions of motion of ion and atom, that is, they are highly effective as momentum-transferring collisions between the ionized and neutral components of the plasma. The cross-section for the charge-exchange process, according to the calculations of Dalgarno and Yadav (1953), is approximately $50\ \pi\ a_0^2$. In addition, there is true elastic scattering, and we may roughly calculate its cross-section by using the adiabatic approximation and the potential curves for the H_2^+ molecular ion given by Bates, Ledsham, and Stewart (1953). If we assume the potential $U(r)$ to have a simple r^{-6} dependence and integrate the momentum transfer along the straight line that represents the zero-order approximation to the orbit, we find that $q(\theta)$, the cross-section for scattering by an angle of θ or greater, is given by

$$q(\theta) = \pi p^2 , \tag{44}$$

where

$$U(p) = \frac{16\,\theta E}{15\pi} ; \tag{45}$$

here E is the relative kinetic energy and p is the impact parameter. The numerical coefficient does not depend strongly on the assumed power law, and so we may solve equation (45) with the numerically available potential function for $U(r)$. With $\theta = 1$ radian, the result is $q = \pi\ (6.4a_0)^2$ for the $1s\sigma_g$ state, $q = \pi\ (6.0a_0)^2$ for the $2p\sigma_u$ state, and $q = 40\ \pi\ a_0^2$ for the weighted mean. However, according to Dalgarno and Yadav (1953), almost exactly half of these collisions lead to charge-exchange, so the correct cross-section for elastic scattering without charge-exchange is $q = 20\ \pi\ a_0^2$. Furthermore, of the other half, the charge-exchange collisions, a considerable fraction, say half, must be collisions with the very large angle of scattering, near 180°. In such collisions the nuclei exchange considerable momentum, but the net result after the collision is a hydrogen atom and a proton with very nearly the same momenta that the hydrogen atom and proton had before the collision, so these are not effective collisions. Therefore, about $10\ \pi a_0$ must be subtracted from the charge-exchange cross-section to allow for the ineffective collisions, and the final result is $q = (50 - 10) + 20\ \pi a_0^2 = 60\ \pi a_0^2 = 5 \times 10^{-15}$ cm^2.

In the collisions between He and H^+, charge-exchange cannot occur, and the elastic scattering cross-section can be found by the method described above for $H + H^+$. The potential curve L of Coulson and Duncanson (1938) was used, and the resulting cross-section is $q = \pi(2.9a_0)^2 = 8 \times 10^{-16}$ cm^2.

For the collisions $H + M^+$ and $He + M^+$ in the photosphere, the necessary potential curves are not available, but we may crudely estimate the cross-section to have the same order of magnitude as the $H + H^+$ and $H + He^+$ elastic-scattering cross-sections, namely, $q = 8 \times 10^{-16}$ cm^2.

In applying equation (42) to calculate the frictional damping length ζ_2 in the chromosphere, the average collision time for both the $H^+ + H$ and $H^+ + He$ collisions can be found by using the equation

$$\frac{\eta}{\tau_n} = \frac{\eta_1}{\tau_1} + \frac{\eta_2}{\tau_2}, \tag{46}$$

which can easily be derived for $2\pi\nu\tau_1 \ll 1$, $2\pi\nu\tau_2 \ll 1$, where η_1 and η_2 are the ratios of mass densities of two different types of neutral atoms (hydrogen and helium in our case) to the mass density of ions, and τ_1 and τ_2 are the mean times of collision of each type of atom with the ions. With the cross sections given above,

$$\tau_1 = \frac{2.2 \times 10^8}{N_i}, \qquad \tau_2 = 21\,\tau_1, \qquad \text{(sec)} \tag{47}$$

TABLE 7

ALFVÉN-WAVE FRICTIONAL DAMPING LENGTH

HEIGHT h (km)	LOG N_P (cm^{-3})	LOG Nm (cm^{-3})	n	$1/\tau$ (sec^{-1})	ζ_2 (km)	
					$B=2$ gauss	$B=50$ gauss
− 400	14 8	13 3	$\gg 1$	$2\ 0\times10^{6}$	$2\ 8\times10^{6}$	$7\ 0\times10^{7}$
− 300	13 3	13 0	$\gg 1$	$7\ 7\times10^{4}$	$1\ 3\times10^{5}$	$3\ 3\times10^{6}$
− 200	12 5	12 7	$\gg 1$	$1\ 5\times10^{4}$	$3\ 9\times10^{4}$	$9\ 8\times10^{5}$
− 100	11 2	12 3	$\gg 1$	$1\ 7\times10^{3}$	$7\ 4\times10^{3}$	$1\ 9\times10^{5}$
0	9 8	12 0	$\gg 1$	$9\ 3\times10^{2}$	$6\ 6\times10^{3}$	$1\ 7\times10^{5}$
+ 250	10 4	11 4	$\gg 1$	$3\ 1\times10^{2}$	$5\ 0\times10^{3}$	$1\ 2\times10^{5}$
+ 500	10 6	10 7	$\gg 1$	$1\ 8\times10^{2}$	$6\ 3\times10^{3}$	$1\ 6\times10^{5}$
+ 750	10 7	10 1	$\gg 1$	$1\ 7\times10^{2}$	$1\ 2\times10^{4}$	$3\ 1\times10^{5}$
+1000	10 7	9 5	$\gg 1$	$1\ 7\times10^{2}$	$2\ 5\times10^{4}$	$6\ 2\times10^{5}$
+1500	10 5	8 5	88	$1\ 0\times10^{2}$	$5\ 0\times10^{4}$	$1\ 2\times10^{6}$
+2000	10 4	7 6	14	$8\ 4\times10$	$1\ 2\times10^{5}$	$3\ 0\times10^{6}$
+3000	10 2	6 9	3 8	$5\ 0\times10$	$1\ 9\times10^{5}$	$4\ 7\times10^{6}$
+4000	10 0	6 5	1 8	$2\ 6\times10$	$1\ 9\times10^{5}$	$4\ 8\times10^{6}$
+5000	9 8		0 76	$1\ 0\times10$	$1\ 9\times10^{5}$	$4\ 7\times10^{6}$
+6000	9 6		0 46	3 2	$1\ 1\times10^{5}$	$2\ 7\times10^{6}$

(note that, on the average, a hydrogen atom loses half its momentum in a collision with a proton, while a helium atom loses one-fifth of its momentum) and the degree of ionization of hydrogen has been taken from van de Hulst (1953), while helium has been assumed to be mostly neutral throughout the chromosphere and to have an abundance ratio $(N(\text{He})/N(\text{H}) = 0.10$. In the photosphere the mean-free time of a neutral atom is determined by the number of collisions with both hydrogen and metallic ions, but, since hydrogen is mostly neutral, the ratio of numbers of hydrogen and helium atoms is constant, and the average collision time is

$$\frac{1}{\tau_n} = \frac{N_i}{3.0 \times 10^8} + \frac{N_m}{1.1 \times 10^9} \qquad (\text{sec}^{-1}),$$

where N_m is the number of metallic ions. The results of these calculations are summarized in Table 7, where again the damping lengths have been calculated for the frequency $\nu_0 = 1.2 \times 10^{-2}$ sec^{-1}.

Inspection of Tables 6 and 7 shows that in the undisturbed disk, with a representative

field of $B = 2$ gauss, the Joule heating mechanism is the dominant dissipation process below 1000 km, while above this level the frictional damping is most important. The damping is very great in the photosphere and the low chromosphere below 500 km height; so any Alfvén waves generated in the hydrogen convection zone would surely be completely absorbed long before reaching the surface of the sun. The same conclusion applies to slow-mode waves, which are essentially Alfvén waves at these depths. The physical reason for the great damping is that the Alfvén-wave velocity is very small (because of the high density), the wave length is consequently quite short, and the wave dissipation, which depends on gradients of the field quantities, is consequently large. At heights above 1000 km in the chromosphere, the damping length rapidly becomes larger than the remaining height above, and consequently only relatively small fractions of any energy flux carried by Alfvén waves can be absorbed at these levels. The damping lengths both depend on the wave frequency in the same way, and at the extreme high-frequency end of the spectrum generated in the hydrogen convection zone, where $\nu = \nu_{\max} = 4\nu_0$, the damping lengths become smaller by a factor of 16, and so about 30 per cent of the flux at this frequency incident at the height 2000 km would be absorbed in the chromosphere; but, in general, the heating effect of the Joule and frictional damping mechanisms is small.

This conclusion differs from that of Piddington (1956) for two reasons. First, the atom-ion collision cross-sections estimated above are large in comparison with the value $q = 2.3 \times 10^{-16}$ cm^2 adopted by Piddington from the extrapolation of calculated cross-sections for protons with energies above 90 ev, together with experimental data on low-energy atom-atom collisions, and the larger cross-sections decrease the phase lag between the motions of the atoms and ions and hence decrease the dissipation. Second, the frequency spectrum derived in Section IV above is considerably lower in frequency and wider than the spectrum used by Piddington to estimate the dissipation, namely, a band between $\nu_{\min} = 0.016$ and $\nu_{\max} = 0.048$ sec^{-1}.

In the plage areas, with a representative magnetic field of 50 gauss, the Alfvén velocity is larger, and the damping is therefore smaller, as Tables 6 and 7 show. The variation of the Joule heating process with the strength of the magnetic field is greater than the variation of the frictional process, and for this reason the latter process is more important in plage areas for all heights in the chromosphere above 250 km. In the photosphere the damping is small enough that a fraction, of the order of e^{-1}, of any flux there might be in the form of Alfvén waves can penetrate through to the chromosphere, where, however, the damping is so low that essentially all the energy would pass through to the corona.

Now, as has been seen in Section IV, it is expected that only fast-mode waves will be generated in the hydrogen convection zone, and the dissipation of these waves is the most relevant process for the heating of the chromosphere. The full study of the damping of fast-mode waves by viscosity, Joule heating, and frictional processes is extremely complicated (see Lehnert 1959), but, for our purposes, relatively simple estimates are sufficient. In the photosphere $V_S \gg V_A$, and the fast mode is essentially a sound wave, with a damping length given by

$$\zeta_3 = \frac{3\,V_S^3 \rho}{16\pi^2\nu^2\mu}, \tag{48}$$

which is always very long, of the order of 10^7 km for the largest viscosity listed in Table 6; hence the sound damping is completely negligible, a very well-known result used by Biermann (1948) and Schwarzschild (1948). Therefore, it is only the electromagnetic processes that are important in damping the fast-mode waves, but these processes can be effective only when the waves have become essentially hydromagnetic in character, that is, at heights for which $V_A \geq V_S$. We have already seen that, at these heights, above 2000 km in the undisturbed sun and above 500 km in the plage areas, the damping of

Alfvén waves is small. Therefore, the fast-mode waves suffer essentially no dissipation by the Joule heating and functional processes, and the main dissipative effects must occur after the waves have built up to finite-amplitude disturbances. The physical reason is that the fast-mode waves always have a sufficiently high velocity that the wavelength is large for the frequencies that occur in the sun and the dissipation is correspondingly small.

VII. DISSIPATION OF SHOCKS

In the previous section the dissipative mechanisms that occur for small-amplitude continuous waves were discussed and found to be insufficient to remove more than a fraction of the energy transported into the chromosphere by the waves. However, as they run out, their amplitudes build up, and shock fronts or near-discontinuities develop, increasing the dissipation very greatly. The same kind of microscopic collision processes as in the case of small-amplitude waves are responsible for the damping but at a greatly enhanced rate in the narrow transition zone at the shock front, with its steep gradients of density and temperature. The most straightforward way to evaluate this dissipation would be to work out in a detailed way the structure of the shock front, but this is a complicated and difficult problem even for pure gas-dynamic shocks (see Lighthill 1958), and only some general results are available for magnetohydrodynamic disturbances (Marshall 1955).

The alternative method for evaluating the dissipation, due to Brinkley and Kirkwood (1947) and applied to the gas-dynamic waves in the chromosphere by Schatzman (1949) and Weymann (1960), makes use of the fact that the irreversible processes all occur at the discontinuous shock front, so that their effect can be estimated purely from the strength of the shock, together with a simple assumption about the return behind the front to the original equilibrium state. On the other hand, the energy carried by the disturbance can also be expressed in terms of the shock strength, together with an assumption about the form of the wave, so in this way the dissipation can be related to the energy transported. Thus a combination of thermodynamic reasoning with fairly plausible assumptions circumvents the necessity of explicitly working out the details of the dissipative processes in the shock transition zone. This method was developed by Brinkley and Kirkwood (1947) to apply to relatively weak shocks and was found by them to give good agreement with experimental data for shocks in air and water. We shall use the method generalized to magnetohydrodynamic waves, and, though the shocks that occur in the chromosphere are weak, so that the theory would be applicable if they were pure gas-dynamic shocks, the extension to include magnetohydrodynamic effects has never been subjected to an experimental test. It is probably not true in detail, particularly when the magnetic effects are large, but it seems sufficient for a first survey of the dissipation of shock waves in the sun.

We shall use the results and notation of Bazer and Ericson (1959) to treat the fast-mode shocks (symbolized by these authors as M_f shocks) of interest in the photosphere and chromosphere. The undisturbed gas ahead of the front has density, pressure, and magnetic field ρ_0, P_0, and $\boldsymbol{B}_0$, which change discontinuously across the front to ρ_1, P_1, and $\boldsymbol{B}_1$, and the strength of the shock is measured by the jump in density $\rho_1 - \rho_0 = \bar{\eta}\rho_0$. The velocity ahead of the front vanishes, while behind the front it is $\boldsymbol{u}_1$, and behind the front all the quantities ρ, P, $\boldsymbol{B}$, and $\boldsymbol{u}$ vary continuously from their peak values ρ_1, P_1, $\boldsymbol{B}_1$, and $\boldsymbol{u}_1$ at the front, to their equilibrium values ρ_0, P_0, $\boldsymbol{B}_0$, and 0 far behind. The available mechanical energy D carried per unit cross-section areas by the disturbance can then be expressed in terms of an integral over the excess pressure and magnetic field at time t after the passage of the shock:

$$D = -\int_0^\infty \left\{ u_n \left[(P - P_0) + \frac{1}{8\pi}(B^2 - B_0^2) \right] - \frac{1}{4\pi}\, \boldsymbol{u} \cdot (B_n \boldsymbol{B} - B_{n0}\boldsymbol{B}_0) \right\} dt . \qquad (49)$$

Here u_n stands for the component of velocity in the direction normal to the front, measured positive in the direction of mass flow across the front (so the velocity of the matter behind the front is negative in this co-ordinate system, which is the reason for the minus sign in front of the whole integral); B_n stands for the same component of the magnetic field, while u_y and B_y (used in the next equation) stand for the components of these vectors normal to the front, in the plane defined by the normal and B_0. Since B_n is continuous across the front, this expression can also be written

$$D = -\int_0^\infty \left\{ u_n \left[(P - P_0) + \frac{1}{8\pi}(B^2 - B_0^2) \right] - \frac{1}{4\pi} u_y B_n (B_y - B_{y0}) \right\} dt , \tag{50}$$

or, in terms of quantities just behind the shock,

$$D = -\int_0^\infty \left\{ u_{n1} \frac{u_n}{u_{n1}} \left[(P_1 - P_0) \frac{(P - P_0)}{(P_1 - P_0)} + \frac{1}{8\pi} (B_1^2 - B_0^2) \frac{(B^2 - B_0^2)}{(B_1^2 - B_0^2)} \right] \right. \tag{51}$$

$$\left. - \frac{1}{4\pi} u_{y1} \frac{u_y}{u_{y1}} B_n (B_{y1} - B_{y0}) \frac{(B_y - B_{y0})}{(B_{y1} - B_{y0})} \right\} dt .$$

Our basic assumption, then, is that

$$\frac{u_n}{u_{n1}} \frac{(P - P_0)}{(P_1 - P_0)} , \qquad \frac{u_n}{u_1} \frac{(B^2 - B_0^2)}{(B_1^2 - B_0^2)} \qquad \text{and} \qquad \frac{u_y}{u_{y1}} \frac{(B_y - B_{y0})}{(B_{y1} - B_{y0})}$$

all have the same time dependence, $f(t)$, so that we can write

$$D = -\left\{ u_{n1} \left[(P_1 - P_0) + \frac{1}{8\pi} (B_1^2 - B_0^2) \right] - \frac{1}{4\pi} u_{y1} B_n (B_{y1} - B_{y0}) \right\} \int_0^\infty f(t)\, dt \tag{52}$$

$$= -\left\{ u_{n1} \left[(P_1 - P_0) + \frac{1}{8\pi} (B_1^2 - B_0^2) \right] - \frac{1}{4\pi} u_{y1} B_n (B_{y1} - B_{y0}) \right\} t_0 .$$

Now we can use the results of Bazer and Ericson (1959) to express all the variables inside brackets in equation (52) in terms of the shock strength $\bar{\eta}$, the angle θ between the initial magnetic field $\boldsymbol{B}_0$ and the normal to the front, and the density, sound velocity, Alfvén velocity, and fast-mode velocity ρ_0, V_S, V_A, and V_f, respectively, in the undisturbed gas just ahead of the front, and the result is

$$D = \rho_0 V_F \bar{\eta}^2 t_0 \left[V_S^2 + V_A^2 \frac{\sin^2 \theta}{(1 - V_A^2 \cos^2 \theta / V_F^2)^2} + \ldots \right] . \tag{53}$$

This expression has been derived for weak shocks; in the same approximation,

$$\begin{aligned} P_1 - P_0 &= \gamma \bar{\eta} P_0 + \ldots , \\ B_{y1} - B_{y0} &= \frac{\sin \theta}{(1 - V_A^2 \cos^2 \theta / V_F^2)} \bar{\eta} B_0 + \ldots , \\ u_{n1} &= -\bar{\eta} V_F + \ldots , \\ u_{y1} &= \frac{\sin \theta \cos \theta}{(1 - V_A^2 \cos^2 \theta / V_F^2)} \bar{\eta} \frac{V_A^2}{V_F^2} + \ldots , \end{aligned} \tag{54}$$

and these expressions, as well as equation (53), are actually only the first terms of power series but are fairly good approximations for $\bar{\eta} < 1$.

Next we calculate the dissipation caused by the rapid irreversible comparison at the front, followed by the continuous variation behind it. Following Weymann (1960), for this calculation we idealize the changes that an element of material undergoes as first, instantaneous compression from the equilibrium pressure and density P_0, ρ_0 to the peak pressure and density behind the front P_1, ρ_1; second, rapid cooling at constant density to the state P^*, ρ_1, at which the entropy has decreased to the same value it had before the compression (this stage is meant to represent the rapid radiative cooling of the heated material just behind the front); finally, slower adiabatic expansion (without heat exchange with its surroundings) to the final equilibrium state P_0, ρ_0, identical with the initial state. The energy dissipation, which all occurs during the second stage, can be directly evaluated from the pressure and density variations, but it is simplest to use the expression for the entropy jump per unit mass ΔS across the front given by Bazer and Ericson (1959),

$$\Delta S = \frac{\gamma(\gamma-1)\,c_v}{4}\left[\tfrac{1}{3}(\gamma+1) + \frac{V_A^2 \sin^2\theta}{V_S^2(1 - V_A^2\cos^2\theta/V_F^2)^2}\right]\bar{\eta}^3 + \ldots, \tag{55}$$

where c_v is the specific heat at constant volume. Then, since the entropy charge in the third, adiabatic stage is zero but at the end of it the material has returned to its initial state, the entropy change in the second, cooling stage must be just the negative of that given by equation (55). Now the change in internal energy e per unit charge in entropy, at constant density is

$$\left(\frac{\partial e}{\partial S}\right)_\rho = \frac{1}{c_v(\gamma-1)}\frac{P}{\rho} \tag{56}$$

(Courant and Friedrichs 1948), so the energy lost per unit mass during the cooling stage is

$$\Delta e = \frac{\gamma P \bar{\eta}^3}{4\rho}\left[\tfrac{1}{3}(\gamma+1) + \frac{V_A^2 \sin^2\theta}{V_S^2(1 - V_A^2\cos^2\theta/V_F^2)^2}\right] + \ldots, \tag{57}$$

where P and ρ are mean pressures and densities that occur during this stage. However, since this treatment is intended for weak shocks and we are consistently keeping only the first non-zero term, P, ρ can be replaced by P_1, ρ_1, or, most simply, by P_0, ρ_0. Then, finally, the energy loss per unit length traversed by the shock, and per unit area of the shock, is

$$\begin{aligned}\frac{dD}{ds} &= -\rho_0 \Delta e \\ &= -\frac{\rho_0 \bar{\eta}^3}{4}\left[\tfrac{1}{3}(\gamma+1)\,V_S^2 + \frac{V_A^2 \sin^2\theta}{(1 - V_A^2\cos^2\theta/V_F^2)^2}\right] + \ldots,\end{aligned} \tag{58}$$

or, using equation (53) for D, the energy per unit area carried by the shock, the mean damping length ζ for a fast-mode shock is given by

$$\begin{aligned}\frac{1}{\zeta} &= -\frac{1}{D}\frac{dD}{ds} \\ &= \frac{\bar{\eta}}{4 V_F t_0}\left[\frac{(\gamma+1)\,V_S^2/3 + V_A^2 \sin^2\theta/(1 - V_A^2\cos^2\theta/V_F^2)^2}{V_S^2 + V_A^2 \sin^2\theta/(1 - V_A^2\cos^2\theta/V_F^2)^2}\right] + \ldots.\end{aligned} \tag{59}$$

Since, for a monatomic gas $\gamma = \frac{5}{3}$ and $(\gamma + 1)/3 = \frac{8}{9}$, it is not a bad approximation at all to replace the bracketed expression in equation (59) by 1, and to use for the damping length the simple formula

$$\zeta = \frac{4 V_F t_0}{\bar{\eta}}. \tag{60}$$

Thus the damping length of a fast-mode magnetohydrodynamic shock depends chiefly on its velocity, the effective time required for it to pass a point, and its strength, measured by the density jump (or, in other words, the compression caused by the passage of the front).

Radiative cooling and also partial ionization tend to reduce the effective value of γ, but, even with the limiting isothermal value $\gamma = 1$, $(\gamma + 1)/3 = \frac{2}{3}$, and our approximation is not too bad. Actually, however, as Weymann (1960) has shown, if the cooling at the front is so strong that the wave behind it is completely isothermal, then the damping length has a different form, independent of $\bar{\eta}$. In the sun, the radiative cooling in the photosphere above $\tau = 1$ is so effective that this isothermal case is probably reached, while deeper down in the hydrogen convection zone the situation is more nearly adiabatic (Spiegel 1957). In the chromosphere many observations suggest that temperature fluctuations occur, with lifetimes of several minutes (De Jager 1959*b*), so here again radiative cooling is not completely effective, probably because a considerable fraction of the radiation is concentrated in optically thick emission lines and also because the recombination time is long. We have therefore consistently used equation (60) to calculate the dissipation, but it would be instructive to repeat the computations, assuming completely isothermal conditions behind the shocks, at least in the photosphere and very low chromosphere.

Now equation (60), though it correctly predicts an infinite damping length as the strength goes to zero, is not really applicable to very small-amplitude waves because, in the derivation, a shock or discontinuity was assumed, while the small-amplitude waves are produced and initially propagate as continuous disturbances, which may be schematized as sinusoidal sound waves. The shock develops in the well-known way described in many textbooks (for instance, Sommerfeld 1950), because the crest with maximum positive perturbation velocity u runs forward with this speed with respect to the wave, while the trough with maximum negative perturbation velocity runs backward with the same speed, and they thus approach each other with a velocity $2u$. The distance between the crest and trough is initially $\lambda/2$; so, for a wave in a homogeneous medium, the time required for the maximum and minimum of velocity to meet and form a discontinuous shock front is $\lambda/4u$. For a wave propagating out in the solar atmosphere, the velocity amplitude increases because of the decreasing density. In the very simplest approximation we may neglect dissipation, take the velocity of sound V_S (and hence also the wavelength λ) to be constant, and assume that the density falls with a scale height H, so the perturbation velocity can be written

$$u = u_0 \exp\left(\frac{z}{2H}\right),$$

where here z is the height measured from an arbitrary zero point in the solar atmosphere. If the wave propagates at an angle ϕ to the vertical, the time required for the trough and crest to meet and form a discontinuity and the velocity amplitude at that time are given by the solutions to the equations

$$\begin{aligned} \int_0^t u\,dt = \frac{\lambda}{4} &= \int_{z_1}^{z} u_0 \exp\left(\frac{z}{2H}\right) \frac{dz}{V_S \cos\phi} \\ &= \frac{2Hu}{V_S \cos\phi}, \end{aligned} \tag{61}$$

where z_1 is the height of emission of the waves, and we have used the fact that exp $(z_1/H) \ll \exp(z/H)$. Thus

$$2u = \frac{V_S \lambda \cos\phi}{4H} = \frac{V_S^2 \cos\phi}{4\nu H}, \tag{62}$$

and, when the shock is developed, $2u$ is the total jump in velocity across the shock, given by $\bar{\eta} V_S$ for weak shocks. Therefore,

$$\bar{\eta}_1 = \frac{V_S \cos\phi}{4\nu H} = 0.68 \cos\phi \tag{63}$$

gives the strength $\bar{\eta}_1$ at which the shock is fully developed (the numerical values are $\nu = 1.2 \times 10^{-2}$ sec, $V_S = 6.5$ km/sec, $H = 200$ km, appropriate at a height of about $h = 1000$ km in the chromosphere). Above this shock strength, equation (60) is applicable, while for smaller strengths the damping length is greater than the formula indicates, although, of course, it does not increase abruptly to infinity, for there must be some dissipation caused by the steepened slope before the wave has become a fully developed shock.

We can now also estimate the characteristic time t_0, defined in terms of the energy transported by a shock front by equation (52). In the case of a pure gas-dynamic shock, equation (53) reduces to

$$D = \rho_0 V_S^3 \bar{\eta}^2 t_0, \tag{64}$$

while the energy flux transported by small-amplitude waves per wave is

$$D = \frac{\rho_0 u^2 V_S}{2\nu} \tag{65}$$

(Lamb 1945). Now the total difference in velocity between crest and trough is $2u$ for the sinusoidal wave and is $\bar{\eta} V_S$ for the weak shock. Therefore, since a sinusoidal disturbance eventually transforms itself into a weak shock with, to the first approximation, no change in amplitude, we find, by comparing equations (46) and (65),

$$t_0 = \frac{1}{8\nu} = 10 \text{ sec} \tag{66}$$

for $\nu = \nu_0 = 1.2 \times 10^{-2}$ sec^{-1}, the mean frequency in the sun. Note that, by considering periodic disturbances, we have essentially treated the transformation of a train of sinusoidal waves into a train of N or saw-tooth waves, while, for a single disturbance or for other different assumptions, a different numerical constant might occur in equation (66); in fact, Schatzman (1949) has used $\frac{1}{4}$, and Weymann (1960) has used $\frac{1}{12}$, instead of our $\frac{1}{8}$. These differences cause only minor changes in the result, however, because of the rapid increase in dissipation with increasing shock strength. It can now be seen from equation (60) that, for a shock strength $\bar{\eta} = 0.5$, the damping length is equal to the wavelength, so that the shocks, once they build up, are much more rapidly dissipated than the small-amplitude waves of the previous section.

Now, finally, our problem is to use the results derived in this section, together with an estimate of the upward flux of energy in the fast-mode waves from Sections II and IV and the ray paths of Section V to analyze the chromospheric heating. It is clear that the most straightforward way to do this would be to study the propagation of individual waves, computing the dissipation along the path of each one, and finally combining all these individual dissipations to find the total non-radiative energy liberated in the chromosphere. This method would involve a considerable amount of numerical work, and so, instead, for a simpler preliminary survey we follow Schatzman (1949) in deriving and

then integrating an approximate equation of transfer for the average total flux carried by all the waves together.

The most difficult part of the problem in either method is a physically correct description of the interaction between shock waves We shall idealize greatly and assume that if two shocks are going in approximately the same direction—that is, with directions of motion differing by less than say 90°—when one overtakes the other, they simply coalesce to form a single stronger shock. On the other hand, when two shocks meet at a large angle between their directions of motion—say greater than 90°—we shall consider the process to be a head-on collision of two shocks. For the moment, in considering the upward transport of energy, we shall ignore these collisions, but we shall return to a discussion of them at the end of this section and in the next section.

In the equation of transfer we first take into account the decrease in the flux due to dissipation. If the upward flux of energy in fast mode of shocks is written πF_+, then the differential equation with dissipation as the only loss is

$$\frac{d(\pi F_+)}{dh} = -\frac{\pi F_+}{\zeta\langle\cos\phi\rangle} = -\frac{\sqrt{(3)}\,\pi F_+}{\zeta} = -\frac{\sqrt{(3)}\,\pi F_+}{4\,V_F t_0}\,\bar{n}\,, \tag{67}$$

where the approximation of equation (60) has been used for the damping length, and $\langle\cos\phi\rangle = 1/\sqrt{3}$ represents the mean value that applies to a radiation field with constant intensity in all upward directions. Actually, of course, in the hydrogen convection zone the correct mean value of the cosine is smaller, because the intensity is largest in the nearly horizontal directions, as discussed in Section IV, while near $h = 0$ the mean is larger because the intensity is peaked in the upward direction; but we shall ignore these improvements and always take

$$\begin{aligned} &\langle\sin\phi\rangle = \sqrt{\tfrac{2}{3}}\,, \qquad \langle\sin^2\phi\rangle = \tfrac{2}{3}\,, \qquad \ldots\,, \\ &\langle\cos\phi\rangle = \sqrt{\tfrac{1}{3}}\,, \qquad \langle\cos^2\phi\rangle = \tfrac{1}{3}\,, \qquad \ldots\,, \end{aligned} \tag{68}$$

for simplicity.

In consistency with the assumption that upward-moving shocks reinforce one another, we shall assume that at any point the average frequency of passage of shocks is ν_0, the same as the mean frequency with which the waves are emitted, so that the average flux at a point can be written

$$\begin{aligned} \pi F_+ &= D\nu\langle\cos\theta\rangle \\ &= \frac{\rho_0 V_F \bar{\eta}^2}{8\sqrt{3}}\left[V_S^2 + \frac{2\,V_A^2}{3(1 - V_A^2/3\,V_F^2)^2}\right], \end{aligned} \tag{69}$$

where we have used equation (53) for D and equation (66) for t_0, with the average values of equation (68). Note we have assumed here that the solar magnetic field is predominantly vertical in the photosphere and chromosphere, so that $\langle\cos^2\theta\rangle = \langle\cos^2\phi\rangle = \frac{1}{3}$, etc.

Weakening by distance, which occurs as a shock produced by a point source spreads out in three dimensions, does not have to be taken into account here because our assumption that shocks catch up with and strengthen each other exactly balances this effect. It would have to be allowed for at distances from the source comparable with the radius of curvature of the sun; but, since these calculations apply only to the chromosphere, a few thousand miles thick, the problem is essentially one-dimensional, and the distance effect is negligible.

However, the effect of refraction, which prevents rays originally emitted in directions making large angles with the vertical from reaching great heights, must be taken into

account (Schatzman 1949). We can introduce it into the differential equation by noticing that in the optical analogy, in the absence of dissipation, the quantity I/n^2 is constant along a ray, where I is the intensity and n is the relative index of refraction. If we set $n = 1$ at the level where the waves are emitted, as in equation (38), then, for a radiation field with equal intensities in all upward directions,

$$\begin{aligned} \pi F_+ &= \text{constant for } n = \frac{V_0}{V_F} > 1 , \\ \frac{\pi F_+}{n^2} &= \left(\frac{V_F}{V_0}\right)^2 \pi F_+ = \text{constant for } n = \frac{V_0}{V_F} < 1 , \end{aligned} \tag{70}$$

give the effect of refraction alone. Thus, combining equations (67) and (70) the differential equation for the net flux is

$$\begin{aligned} \frac{d}{dh}(\pi F_+) &= -\frac{\sqrt{(3)}\,\pi F_+}{4 V_F t_0}\,\bar{\eta} \qquad \text{for } V_F > V_0 , \\ \frac{d}{dh}\left(\frac{V_F^2}{V_0}\,\pi F_+\right) &= -\frac{\sqrt{3}}{4}\,\frac{V_F^2}{V_0^2}\,\frac{\pi F_+}{V_F t_0}\,\bar{\eta} \qquad \text{for } V_F > V_0 , \end{aligned} \tag{71}$$

with $\bar{\eta}$ defined in terms of the flux by equation (69). For numerical calculations it is simplest to use the auxiliary functions,

$$g_1(h) = \begin{cases} \dfrac{\rho V_F}{8\sqrt{3}}\left[V_S^2 + \dfrac{2 V_A^2}{3(1 - V_A^2/3V_F^2)^2}\right] & \text{for } V_F < V_0 , \\ \dfrac{\rho V_F^3}{V_0^2 8\sqrt{3}}\left[V_S^2 + \dfrac{2 V_A^2}{3(1 - V_A^2/3V_F^2)^2}\right] & \text{for } V_F > V_0 , \end{cases} \tag{72}$$

and

$$g_2(h) = \frac{\sqrt{3}}{4 V_F t_0} \tag{73}$$

in terms of which the differential equation becomes

$$\frac{d}{dh}\left[\ln \bar{\eta}^2 g_1(h)\right] = -\bar{\eta}\, g_2(h) . \tag{74}$$

Now the differential equation (74) applies only when the dissipation by the shock actually occurs, that is, according to the discussion leading up to equation (63), for $\bar{\eta} > \langle\bar{\eta}_1\rangle = 0.68\,\langle\cos\phi\rangle = 0.39$. At smaller shock strengths, the dissipation is less than equation (74) suggests, but not zero, and we can approximately account for this by taking the damping to be identically zero below some strength smaller than 0.39, say 0.30, and applying the full dissipation above that strength. The boundary condition is given by the energy flux incident from below, for which we have adopted, on the basis of the discussions in Sections II and IV, $\pi F_+ = 3 \times 10^7$ ergs/cm^2 sec for the average undisturbed sun. With this value, equation (69) for the flux leads to $\bar{\eta} = 0.32$ as the mean shock strength at the base of the chromosphere, and $h = 0$. This is close enough to the 0.30 mentioned above that the integrations have been started at this point, that is, the boundary condition that has been adopted is $\bar{\eta} = 0.32$ at $h = 0$. The results are not very sensitive at all to this assumption; in fact, one integration was carried out, assuming that

no dissipation occurs for $\bar{\eta} < 0.50$, which, with the same net flux, is reached at a height of about $h = 450$ km in the chromosphere, but at greater heights this solution converges rapidly to the solution begun at $h = 0$.

Numerical solutions for assumed magnetic fields $B = 0.5$ and 2 gauss, to represent the disk of the sun, as well as $B = 50$ gauss, to represent a plage area, were carried out numerically and are listed in Table 8. Also, for the plage field, additional solutions are listed for assumed fluxes $\pi F_+ = 1 \times 10^8$ ergs/cm² sec and 3×10^8 ergs/cm² sec, the last value being the estimated flux in a plage area according to Section IV, and there is one solution for a normal field ($B = 2$ gauss), but a low assumed flux ($\pi F_+ = 3 \times 10^6$ ergs/cm² sec) calculated for comparison purposes. The calculated dissipation per unit mass as a function of height, which must be balanced by the radiation and thus tends to determine the local temperature, is shown graphically for each solution in Figure 2, while the upward energy flux as a function of height is plotted for each solution in Figure 3.

Some general features are common to all the solutions. At first, at the lower heights, the shock strength $\bar{\eta}$ rises, because of the decreasing density and the nearly constant upward flux and velocity of sound. However, the dissipation grows rapidly as the shock strength increases, which, as a result, is limited to a maximum value of about 0.8 over the whole range of tabulated integrations. At greater heights the increase in the wave velocity, due to the increasing importance of magnetohydrodynamic effects, tends both to decrease the shock strength (for a given flux) and also to decrease the flux by refraction, and both these effects decrease the dissipation still farther out. The greatest heating (per unit mass) occurs at heights between 1000 and 2000 km in the chromosphere for the magnetic fields 0.5 and 2 gauss assumed to apply, on the average, to the sun. Now if the equilibrium at a given height in the chromosphere were independent of density, then the relative number of atoms and ions in excited states and able to emit radiation would depend only on temperature, and the emission rate per unit mass would also depend only on temperature, and therefore the maximum temperature would occur between 1000 and 2000 km. However, particularly at the low densities occurring in the outer part of the chromosphere, the equilibrium is strongly density-dependent, and most radiation processes are a consequence of two-body collisions; hence it is the heating rate per unit mass and per unit density that fixes the temperature (Athay and Thomas 1956). This quantity continues to increase outward beyond 2000 km, eventually nearly flattening off from 4000 to 6000 km, and these calculations therefore predict that the chromospheric temperature continues to increase (or at least does not decrease) outward to the boundary of the corona.

In the plage regions the magnetohydrodynamic effects become important at smaller heights in the chromosphere, and, as a result, the shock strength is smaller, and the dissipation is concentrated to smaller heights, with a maximum height (per unit mass) between 500 and 750 km. However, the increased refraction is a little less effective than the decreased dissipation, and, as a result, the remaining upward flux at a given large height increases with increasing magnetic field, for the same initial flux at the bottom of the chromosphere (compare solutions 1, 2, and 5). Furthermore, the increased upward flux in the plage regions causes the shock strength to be large lower down and therefore causes dissipation to occur at depths down to -200 km in the photosphere (see solutions 6 and 7).

The effect of refraction naturally decreases with decreasing magnetic field, and integration of the dissipation tabulated in Table 8 gives the result that, at $B = 0.5$ and 2 gauss, essentially all the wave energy entering the chromosphere is absorbed there, and only a negligible amount is refracted, while, for $B = 50$ gauss, about 78 per cent is dissipated, and 22 per cent is refracted back down into the photosphere, for the solution with flux 3×10^7 ergs/cm² sec incident from below, and for larger fluxes the fraction dissipated is larger, reaching 98 per cent for the flux 3×10^8 ergs/cm² sec incident from be-

TABLE 8

MEAN SHOCK STRENGTH, ENERGY FLUX, AND DISSIPATION FOR FAST-MODE WAVES

HEIGHT h (km)	MEAN SHOCK STRENGTH $\bar{\eta}$	FLUX πF_+ (ergs/cm² sec)	DISSIPATION ϵ (ergs/cm³ sec)	DISSIPATION ϵ/ρ (ergs/gm sec)
	1 $B=0.5$ gauss, $\pi F_+(0)=3\times10^7$ ergs/cm² sec			
0	0.32	3.0×10^7	6.4×10^{-1}	4.0×10^7
250	41	1.5×10^7	3.9×10^{-1}	8.3×10^7
500	62	7.2×10^6	2.8×10^{-1}	3.0×10^8
750	71	2.6×10^6	1.1×10^{-1}	4.7×10^8
1000	78	8.1×10^5	3.9×10^{-2}	6.5×10^8
1500	74	8.2×10^4	3.6×10^{-3}	6.0×10^8
2000	68	1.1×10^4	4.0×10^{-4}	5.3×10^8
3000	32	8.0×10^2	1.2×10^{-5}	8.0×10^7
4000	19	1.8×10^2	1.3×10^{-6}	2.2×10^7
5000	12	6.4×10	2.2×10^{-7}	9.0×10^6
6000	0.078	3.1×10	6.5×10^{-8}	4.7×10^6
	2. $B=2$ gauss, $\pi F_+(0)=3\times10^7$ ergs/cm² sec			
0	0.32	3.0×10^7	6.4×10^{-1}	4.0×10^7
250	43	1.6×10^7	4.5×10^{-1}	9.5×10^7
500	61	7.1×10^6	2.8×10^{-1}	2.9×10^8
750	70	2.5×10^6	1.1×10^{-1}	4.6×10^8
1000	78	8.1×10^5	3.8×10^{-2}	6.4×10^8
1500	72	8.8×10^4	3.7×10^{-3}	6.1×10^8
2000	55	1.6×10^4	4.1×10^{-4}	5.5×10^8
3000	12	1.1×10^3	3.2×10^{-6}	2.1×10^7
4000	058	4.6×10^2	4.2×10^{-7}	7.0×10^6
5000	029	1.5×10^2	4.4×10^{-8}	1.8×10^6
6000	0.018	7.8×10	9.7×10^{-9}	8.1×10^5
	3 $B=2$ gauss, $\pi F_+(0)=3\times10^7$ ergs/cm² sec No Dissipation for $\bar{\eta}\leq0.50$			
0	0.32	3.0×10^7	. .	. . .
250	58	3.0×10^7	1.1	2.4×10^8
500	75	1.0×10^7	5.0×10^{-1}	5.3×10^8
750	79	3.2×10^6	1.6×10^{-1}	6.4×10^8
1000	83	9.1×10^5	4.6×10^{-2}	7.6×10^8
1500	73	9.0×10^4	3.8×10^{-3}	6.3×10^8
2000	55	1.7×10^4	4.2×10^{-4}	5.6×10^8
3000	12	1.1×10^3	3.2×10^{-6}	2.1×10^7
4000	058	4.2×10^2	4.2×10^{-7}	7.0×10^6
5000	029	1.5×10^2	4.4×10^{-8}	1.8×10^6
6000	0.018	7.8×10	9.7×10^{-9}	8.1×10^5
	4. $B=2$ gauss $\pi F_+(0)=3\times10^6$ ergs/cm² sec			
0	0.10	3.0×10^6		
250	18	3.0×10^6	. . . .	. . .
500	37	2.6×10^6	6.1×10^{-2}	6.5×10^7
750	51	1.3×10^6	4.1×10^{-2}	1.7×10^8
1000	64	5.4×10^5	2.1×10^{-2}	3.5×10^8
1500	68	7.6×10^4	3.0×10^{-3}	4.9×10^8
2000	.54	1.6×10^4	3.9×10^{-4}	5.2×10^8
3000	12	1.1×10^3	3.0×10^{-6}	2.0×10^7
4000	057	4.3×10^2	3.8×10^{-7}	6.3×10^6
5000	029	1.5×10^2	4.3×10^{-8}	1.8×10^6
6000	0.017	7.6×10	9.6×10^{-9}	8.0×10^5

TABLE 8—*Continued*

Height h (km)	Mean Shock Strength $\bar{\eta}$	Flux πF_+ (ergs/cm² sec)	Dissipation ϵ (ergs/cm³ sec)	Dissipation ϵ/ρ (ergs/gm sec)
	5 $B=50$ gauss, $\pi F_+(0)=3\times10^7$ ergs/cm² sec			
0	0 32	$3\ 1\times10^{7}$	$6\ 5\times10^{-1}$	$4\ 1\times10^{7}$
250	41	$1\ 7\times10^{7}$	$4\ 4\times10^{-1}$	$9\ 4\times10^{7}$
500	51	$9\ 0\times10^{6}$	$2\ 5\times10^{-1}$	$2\ 7\times10^{8}$
750	32	$3\ 4\times10^{6}$	$4\ 0\times10^{-2}$	$1\ 7\times10^{8}$
1000	12	$8\ 3\times10^{5}$	$2\ 0\times10^{-3}$	$3\ 4\times10^{7}$
1500	022	$8\ 4\times10^{4}$	$1\ 2\times10^{-5}$	$1\ 9\times10^{6}$
2000	0046	$1\ 0\times10^{4}$	$1\ 1\times10^{-7}$	$1\ 5\times10^{5}$
3000	0014	$2\ 1\times10^{3}$	$2\ 9\times10^{-9}$	$1\ 9\times10^{4}$
4000	0007	$8\ 4\times10^{2}$	$3\ 7\times10^{-10}$	$6\ 2\times10^{3}$
5000	0003	$3\ 3\times10^{2}$	$4\ 6\times10^{-11}$	$1\ 9\times10^{3}$
6000	0 0002	$1\ 7\times10^{2}$	$9\ 8\times10^{-12}$	$8\ 2\times10^{2}$
	6 $B=50$ gauss, $\pi F_+(-100)=1\times10^8$ ergs/cm² sec			
− 100	0.32	$9\ 8\times10^{7}$	2 1	$4\ 1\times10^{7}$
0	50	$7\ 5\times10^{7}$	2 5	$1\ 5\times10^{8}$
+ 250	56	$3\ 2\times10^{7}$	1 1	$2\ 4\times10^{8}$
+ 500	63	$1\ 3\times10^{7}$	$4\ 6\times10^{-1}$	$4\ 9\times10^{8}$
+ 750	36	$4\ 7\times10^{6}$	$6\ 2\times10^{-2}$	$2\ 6\times10^{8}$
+1000	14	$1\ 1\times10^{6}$	$3\ 0\times10^{-3}$	$5\ 0\times10^{7}$
+1500	025	$1\ 1\times10^{5}$	$1\ 7\times10^{-5}$	$2\ 8\times10^{6}$
+2000	0052	$1\ 3\times10^{4}$	$1\ 6\times10^{-7}$	$2\ 1\times10^{5}$
+3000	0016	$2\ 6\times10^{3}$	$4\ 2\times10^{-9}$	$2\ 8\times10^{4}$
+4000	0008	$1\ 2\times10^{3}$	$6\ 2\times10^{-10}$	$1\ 0\times10^{4}$
+5000	0004	$4\ 2\times10^{2}$	$6\ 7\times10^{-11}$	$2\ 8\times10^{3}$
+6000	0 0002	$2\ 1\times10^{2}$	$1\ 4\times10^{-11}$	$1\ 2\times10^{3}$
	7. $B=50$ gauss, $\pi F_+(-200)=3\times10^8$ ergs/cm² sec			
− 200	0 32	$2\ 8\times10^{8}$	5 8	$4\ 2\times10^{7}$
− 100	48	$2\ 2\times10^{8}$	6 9	$1\ 3\times10^{8}$
0	71	$1\ 5\times10^{8}$	6 8	$4\ 2\times10^{8}$
+ 250	69	$4\ 8\times10^{7}$	2 1	$4\ 4\times10^{8}$
+ 500	71	$1\ 7\times10^{7}$	$6\ 8\times10^{-1}$	$7\ 2\times10^{8}$
+ 750	40	$5\ 6\times10^{6}$	$8\ 1\times10^{-2}$	$3\ 4\times10^{8}$
+1000	15	$1\ 3\times10^{6}$	$3\ 9\times10^{-3}$	$6\ 4\times10^{7}$
+1500	027	$1\ 2\times10^{5}$	$2\ 1\times10^{-5}$	$3\ 6\times10^{6}$
+2000	0056	$1\ 6\times10^{4}$	$2\ 0\times10^{-7}$	$2\ 7\times10^{5}$
+3000	0019	$3\ 1\times10^{3}$	$6\ 0\times10^{-9}$	$4\ 0\times10^{4}$
+4000	0009	$1\ 3\times10^{3}$	$6\ 8\times10^{-10}$	$1\ 1\times10^{4}$
+5000	0004	$5\ 0\times10^{2}$	$8\ 6\times10^{-11}$	$3\ 6\times10^{3}$
+6000	0 0002	$2\ 5\times10^{2}$	$1\ 8\times10^{-11}$	$1\ 5\times10^{3}$

low. Thus the assumption that we have implicitly used—that the wave energy generated in the hydrogen convection zone can be equated to the total energy dissipated in and then radiated from the chromosphere and corona—is approximately verified.

In summary, we have seen in this section that the shock dissipation of fast-mode waves can be worked out and that the heating of the chromosphere can be understood in terms of this process, except that possibly the calculated energy dissipated in the

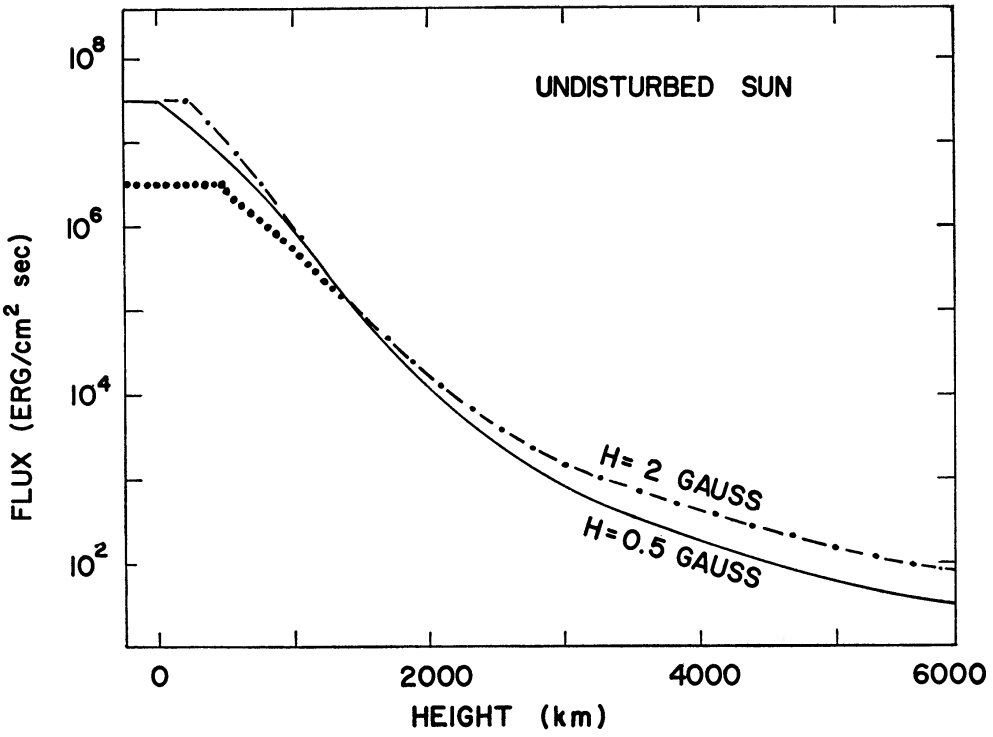

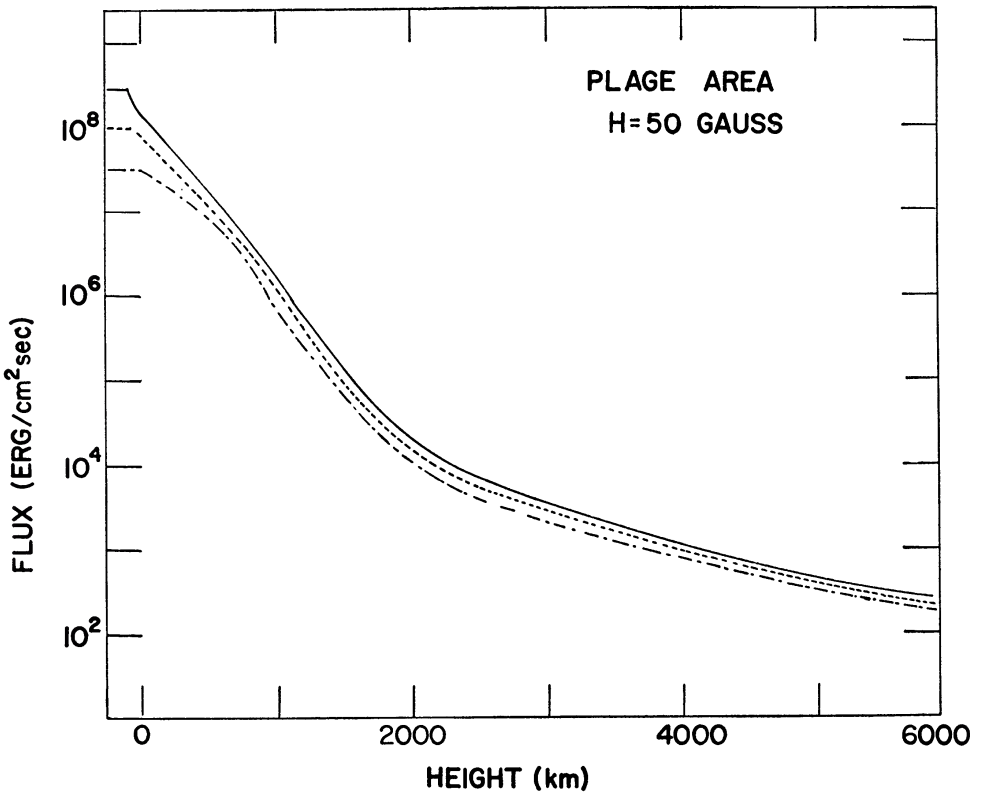

FIG. 2.—Computed fluxes, transported by fast-mode waves in the sun. *Upper*, undisturbed sun: 1, $B = 0.5$ gauss, solid line; 2, $B = 2$ gauss, solid line at left (coincides with 1), alternate dots and dashes at right; 3, $B = 2$ gauss, no dissipation until $\bar{\eta} = 0.50$, alternate dots and dashes (coincides with 1 at right); 4, $B = 2$ gauss, smaller initial flux, dots at left, alternate dots and dashes at right (coincides with 2 and 3). *Lower*, plage area: $B = 50$ gauss, 5, 6, 7 from bottom to top in order of increasing initial flux.

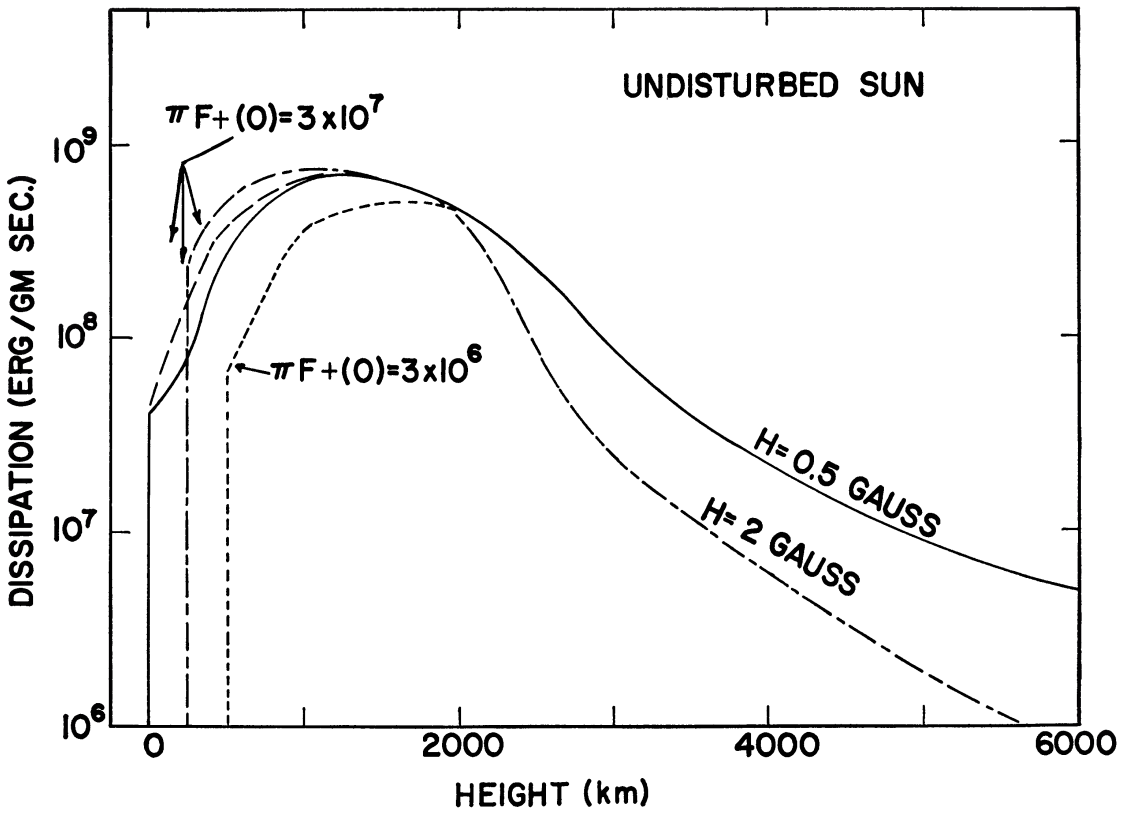

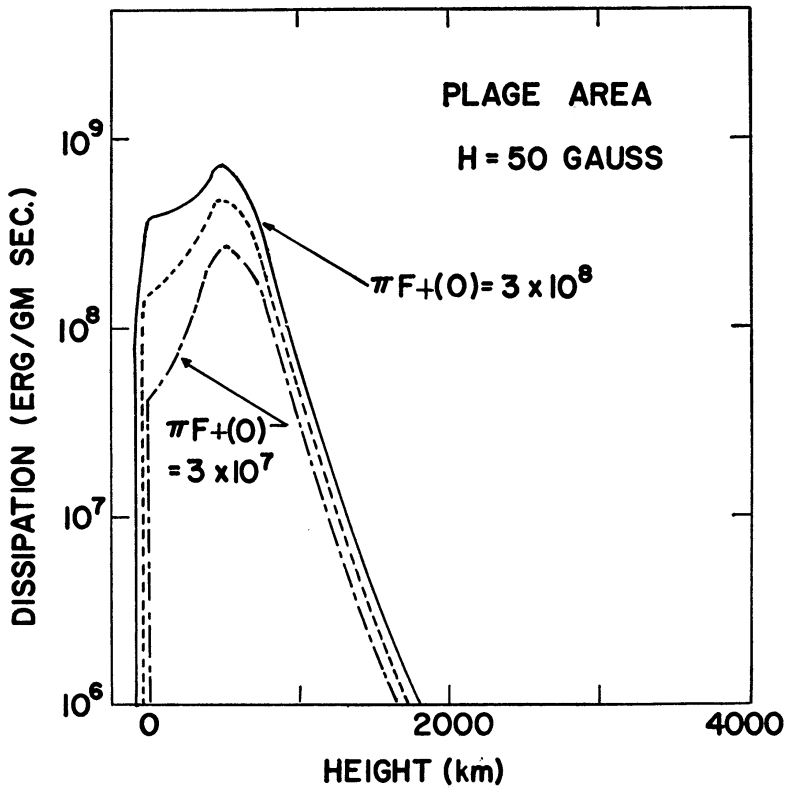

FIG. 3.—Computed dissipation by fast-mode waves in sun. *Upper*, undisturbed sun: 1, $B = 0.5$ gauss, solid line; 2, $B = 2$ gauss, long dashed line at left, alternate long and short dashes at right (coincides with 3); 3, $B = 2$ gauss, no dissipation until $\bar{\eta} = 0.50$, alternate long and short dashes; 4, $B = 2$ gauss, smaller initial flux, short dashes. *Lower*, plage area: $B = 50$ gauss, 5, 6, 7 from bottom to top in order of increasing initial flux.

upper chromosphere is slightly too small. The increased dissipation in plage areas in the chromosphere can be understood as a result of the increased flux incident from below, which also causes excess non-radiative heating in the photosphere below, but not nearly enough to provide the energy source for the photospheric faculae observed at the limb in white light (Ambartsumyan 1958; Rogerson 1961). However, the coronal heating certainly cannot be directly due to the fast-mode waves, simply because the flux incident at the top of the chromosphere is only of order 10^2 ergs/cm^2 sec (see Table 8 or Fig. 3), while the required dissipation in the corona is of order 10^4 or 10^5 ergs/cm^2 sec (see Sec. II). Also, the dissipation of the fast-mode disturbances does not provide enough energy to explain the emission from the upper chromosphere above plage regions.

Now we have omitted from our simplified treatment of the fast-mode waves the effects due to the collisions between shocks, including both increased dissipation and also the generation of additional disturbances. Furthermore, we have not treated in any way the generation of disturbances caused by the passage of fast-mode shocks through the chromosphere. Neither of these processes can be worked out quantitatively at the present time because the required physical theory is not available, but we discuss them qualitatively in the next section and show that it is quite likely that slow-mode disturbances generated in this way provide additional heating in the upper chromosphere and that the Alfvén waves, together with the slow-mode waves, heat the corona. One further question, that could be treated only by a more refined statistical treatment of shocks, is whether it is possible that, in a distribution of shocks, the smallest shocks with therefore the longest dissipation lengths can carry significant amounts of energy to greater heights than the average shocks considered in the differential equation (71).

VIII. ALFVÉN- AND SLOW-MODE WAVES

In the analysis of the preceding section, the interactions between fast-mode shock fronts have been entirely omitted, and we next discuss qualitatively the effects they cause. For overtaking collisions, in which one shock strikes another from behind, it is probably not too bad an approximation simply to add the intensities as we have done; for, at least in the case of pure gas-dynamic waves, the only other effects are a contact discontinuity and a reflected rarefaction wave, which is generally weak (see Courant and Friedrichs 1948) and which therefore can be neglected in the first approximation. However, particularly at the level at which the refraction bends the fast-mode rays toward the horizontal direction, approximately head-on collisions must be common. In such a collision the shock fronts pass through each other, a heated region with a contact discontinuity in it is left between them, and in the magnetohydrodynamic case some energy must, in general, be fed into the other two modes as well, and thus Alfvén-mode and slow-mode disturbances are generated in the collision. This is particularly true in the present case because the head-on collisions occur as a consequence of refraction, which in turn is caused by the increase in the Alfvén velocity outward, and, indeed, reference to Table 2 and Figure 1 shows that, at the levels both in the undisturbed sun and in the plage areas where collisions occur because of refraction, $V_A \approx V_S$ and the mixing between the three modes is a maximum. However, no quantitative basis for calculating the amplitude excited in each mode in such a shock collision is available at the present time. Piddington (1956) has mentioned this effect, referring to it as an interaction of the waves with the observed small-scale inhomogeneities in the structure of the chromosphere, and these inhomogeneities are here identified as the disturbed regions behind the shocks.

Another process in which the Alfvén- and slow-mode disturbances are generated has been discussed by Grad (1959), namely, that the passage of a fast-mode wave in general leaves behind it residues in the other two modes, which then propagate away along the lines of force. Finally, because in the particular case of the chromosphere the wave length of the fast-mode disturbances is of the same order as the dimensions of the layer involved, the approximation of geometrical optics, which is strictly true if the variations

in the medium occur over distances large in comparison with the wavelength, is not well fulfilled. It is therefore plausible that an outward-running fast-mode disturbance will be partly transformed into the other modes, a process that might be called the generation of Alfvén- and slow-mode disturbances by interaction of a fast-mode wave with the large-scale structure of the chromosphere.

From these remarks, it is clear that, particularly at higher levels in the chromosphere, some energy is removed from the fast-mode flux by effects not included in the integrations of the previous section and that this excess is partly dissipated as heat (by shock collisions) and partly fed into the other modes by all three processes mentioned. Further theoretical work on magnetohydrodynamic disturbances will be necessary before the excitation of the various modes can be quantitatively calculated; therefore, we can only indicate, by schematic computations, plausible connections between these expectations and observed features of the sun.

First, for the slow-mode waves, we shall assume that approximately 10 per cent of the fast-mode flux incident at the level where $V_S = V_A$ ($h = 2000$ km in the undisturbed disk with $B = 2$ gauss, 500 km $< h <$ 750 km in the plage regions with $B = 50$ gauss) is converted into upward-traveling disturbances of this type. If much of the excitation is due to the collisions between fast-mode shocks, only a fraction of the sun's disk can be covered at any one time by the slow-mode disturbances, and, guided by observations of spicules, which will be identified below with these disturbances, we shall assume that 10 per cent of the area of the sun is covered by them. Thus, specifically, we assume that above the level $V_S = V_A$ a total of 10 per cent of the area is taken up by slow-mode shocks propagating upward along the assumed vertical field and that at this level the total flux in the slow-mode shocks is approximately 10 per cent of the fast-mode flux, so that, within the area where there is a slow disturbance, the fast-mode and slow-mode fluxes are comparable. The upward-traveling slow-mode shock is discussed by Bazer and Ericson (1959); it is called the 0° limit of an $M_s^{(2)}$ shock under the circumstances we are discussing, $V_S < V_A$, and it is a gas-dynamic shock (G_s shock in their terminology) moving essentially with the speed of sound and with the material motion along the direction of the magnetic field. For very strong disturbances, this goes over continuously into a switch-on shock (S_w) moving with the Alfvén velocity and with material motion perpendicular to the field as well as parallel, but in the chromosphere the waves will not have this property except very near the level where $V_A = V_S$. The slow-mode disturbances can therefore be discussed as pure gas-dynamic or sound shocks, propagating only along the direction of the field, and they can be analyzed by omitting the magnetic-field and refraction effects and the angular dependence of the intensity from the relations of Section VI. Thus the flux πF_{+S} can be written in terms of the mean shock strength $\bar{\eta}_S$:

$$\pi F_{+S} = D_S \nu_S = \rho_0 V_S^3 \bar{\eta}_S^2 t_{0S} \nu_S \,, \tag{75}$$

the damping length ζ_S can be written

$$\zeta_S = \frac{4 V_S t_{0S}}{\bar{\eta}_S} \,, \tag{76}$$

and the differential equation for the flux can be written

$$\frac{d}{dh}(\pi F_{+S}) = -\frac{\pi F_{+S}}{4 V_S t_{0S}} \bar{\eta}_S \,. \tag{77}$$

We have again adopted $t_{0s} \nu_S = \frac{1}{8}$ as for the fast-mode shocks, but, since many of the slow-mode disturbances are, according to the discussion above, generated by collisions of two fast-mode shocks, which certainly occur less frequently than the passage of a single disturbance at a point, it must be that $\nu > \nu_S$ and, correspondingly, $t_{0S} > t_0$. Guided

again by the observations of spicules, we have adopted $t_0 = 100$ and 40 sec, 10 and 2.5 times the characteristic time for fast-mode shocks, in the integrations that follow, two of which were carried out for the undisturbed disk with $B = 2$ gauss and one for a plage area with $B = 50$ gauss (the magnetic field does not enter the differential equation but does determine the starting level, where $V_A = V_S$, and also the initial flux at that level).

The solutions are listed in Table 9, where it should particularly be noted that the flux and dissipation are given within the area covered by slow-mode disturbances. Hence, to find the average of those quantities over the whole solar surface, the tabulated values must be multiplied by the fraction of the surface covered by these disturbances (0.10 according to our assumption). First of all, it can be seen that the average shock strength is quite large in comparison with the fast-mode strength; this is a consequence of the fact that the energy is transported by a relatively ineffective process, namely, the sound mode in regions where $V_S < V_A$. In fact, the shock strengths are large enough that the equations used for the flux and the dissipation, based on the weak-shock approximation, are no longer valid, so that the solutions themselves are only poor approximations and can be trusted only in order of magnitude. The dissipation is relatively ineffective in

TABLE 9

SHOCK STRENGTH, ENERGY FLUX, AND DISSIPATION FOR SLOW-MODE SHOCKS

HEIGHT h (km)	MEAN SHOCK STRENGTH $\bar{\eta}_S$	FLUX πF_{+S} (ergs/cm² sec)	DISSIPATION ϵ (ergs/cm³ sec)	DISSIPATION ϵ/ρ (ergs/gm)
	8. $B=2$ gauss, $t_0=40$ sec			
2000	0 75	$2\ 1\times10^{4}$	$1\ 4\times10^{-4}$	$1\ 8\times10^{8}$
3000	1 02	$1\ 0\times10^{4}$	$8\ 2\times10^{-5}$	$5\ 4\times10^{8}$
4000	0 98	$4\ 8\times10^{3}$	$3\ 4\times10^{-5}$	$5\ 7\times10^{8}$
5000	0 95	$2\ 5\times10^{3}$	$1\ 5\times10^{-5}$	$6\ 3\times10^{8}$
6000	0 92	$1\ 4\times10^{3}$	$7\ 7\times10^{-6}$	$6\ 4\times10^{8}$
	9. $B=2$ gauss, $t_0=100$ sec			
2000	0 75	$2\ 1\times10^{4}$	$5\ 5\times10^{-5}$	$7\ 3\times10^{7}$
3000	1 25	$1\ 5\times10^{4}$	$6\ 0\times10^{-5}$	$4\ 0\times10^{8}$
4000	1 44	$1\ 0\times10^{4}$	$4\ 3\times10^{-5}$	$7\ 1\times10^{8}$
5000	1 57	$6\ 8\times10^{3}$	$2\ 8\times10^{-5}$	$1\ 2\times10^{9}$
6000	1 65	$4\ 4\times10^{3}$	$1\ 8\times10^{-5}$	$1\ 5\times10^{9}$
	10. $B=50$ gauss, $t_0=40$ sec			
750	0 80	$5\ 6\times10^{6}$	$4\ 2\times10^{-2}$	$1\ 8\times10^{7}$
1000	1 38	$4\ 4\times10^{6}$	$5\ 6\times10^{-2}$	$9\ 3\times10^{8}$
1500	2 62	$1\ 8\times10^{6}$	$4\ 1\times10^{-2}$	$6\ 9\times10^{9}$
2000	3 48	$4\ 6\times10^{5}$	$1\ 4\times10^{-2}$	$1\ 9\times10^{10}$
3000	2 12	$4\ 4\times10^{4}$	$7\ 2\times10^{-4}$	$4\ 8\times10^{9}$
4000	1 50	$1\ 1\times10^{4}$	$1\ 2\times10^{-4}$	$2\ 0\times10^{9}$
5000	1 26	$4\ 3\times10^{3}$	$3\ 5\times10^{-5}$	$1\ 5\times10^{9}$
6000	1 12	$2\ 1\times10^{3}$	$1\ 4\times10^{-5}$	$1\ 2\times10^{9}$

reducing the flux because of the long characteristic time assumed (compare solutions 8 and 9), which corresponds physically to a long wave, transporting a large amount of energy, headed by only a single front at which the dissipation chiefly occurs. Also, of course, there is no refraction to reduce the flux. In the upper chromosphere the dissipation in the slow-mode shocks, averaged over the solar surface, is larger than the fast-mode dissipation, as shown in Figure 4, where the presumed best solutions are plotted for the normal sun (solutions 2 and 8) and for a plage area (solutions 7 and 10).

When the upward-propagating slow shocks reach the top of the chromosphere, they excite disturbances in the corona and also themselves carry chromospheric matter up into the corona. It thus appears quite plausible to identify the spicules observed at the limb of the sun as this chromospheric material, carried up along the magnetic lines of force, above the top of the average chromosphere. We can treat the boundary value that arises in an approximate way by considering the slow shock as a pure gas-dynamic shock

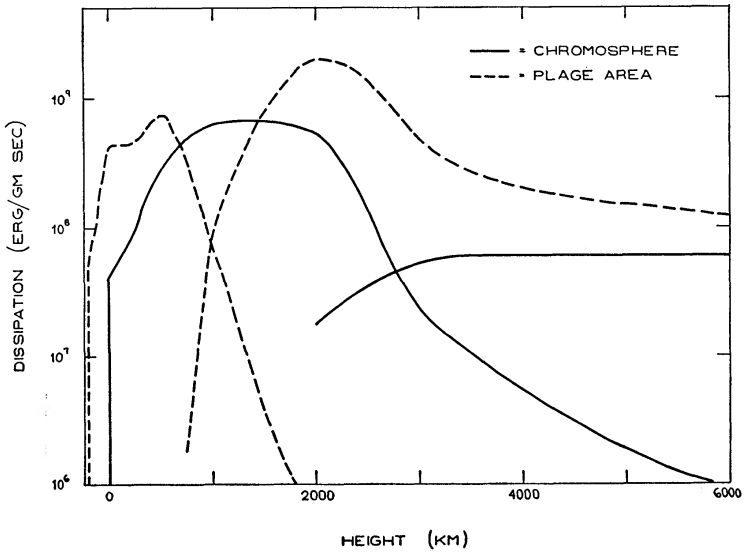

FIG. 4.—Computed dissipation in chromosphere above undisturbed sun, $B = 2$ gauss, *solid line*, solutions 2 and 8, and in plage area, $B = 50$ gauss, *dashed line*, solutions 7 and 10. In both cases left-hand curve is result of fast-mode disturbances; right-hand curve, of slow-mode disturbances (assumed to cover 10 per cent of sun's area at any moment and averaged in this drawing over whole area).

in the corona, as well as a reflected disturbance moving down into the chromosphere, and we shall idealize the transition from the chromosphere to the corona as a sharp interface, plane and perpendicular to the magnetic field and therefore parallel to the incident front. The velocity of sound is much higher in the corona than in the chromosphere; for this computation, we shall treat the disturbances as adiabatic with $\gamma = \frac{5}{3}$ and take the velocities of sound to be $V_S = 12$ km/sec at the top of the chromosphere and $V_S = 160$ km/sec in the corona, corresponding to a temperature of about 1200000° K, while the pressure is assumed constant across the interface. When the shock in the cooler gas strikes the interface, a shock is excited in the hotter gas and runs rapidly ahead, while a rarefaction wave is propagated back into the cooler gas, which is thus speeded up enough that the interface keeps up with the rapidly moving hot gas ahead of it. In the limiting case in which the hotter gas has infinite temperature and therefore (because of the pressure equilibrium) zero density, the problem becomes one of expansion into a vacuum, for which the well-known solution is that the interface moves with the escape speed, three times the speed of sound in the gas behind the rarefaction wave; so we expect that, for a

finite coronal temperature, the speed of the interface will be intermediate between the material velocity behind the shock and the escape speed. Reference to the x-t diagram of Figure 5, together with the relations for shocks and rarefaction waves given by Courant and Friedrichs (1948) (however, the interaction process of a shock in a cooler gas striking a hot gas is incorrectly described in this book), with the definitions

$$y_{ij} = \frac{P_i}{P_j}, \qquad \mu = \frac{\gamma + 1}{\gamma - 1}, \tag{78}$$

give the equations

$$\frac{u_1}{V_0} = \frac{y_{10} - 1}{\sqrt{(\mu y_{10+1})}} \frac{\mu - 1}{\sqrt{(\mu + 1)}}, \tag{79}$$

$$\frac{u_4}{V_3} = \frac{y_{43} - 1}{\sqrt{(\mu y_{43+1})}} \frac{\mu - 1}{\sqrt{(\mu + 1)}}, \tag{80}$$

$$V_1 = \left[\frac{y_{10}(\mu + y_{10})}{\mu y_{10+1}}\right]^{1/2} V_0, \tag{81}$$

$$V_5 = V_1 - \frac{(\gamma - 1)}{2}(u_4 - u_1), \tag{82}$$

$$y_{51} = \left(\frac{V_5}{V_1}\right)^{2\gamma/(\gamma-1)}, \tag{83}$$

$$y_{43} = y_{51} y_{10}. \tag{84}$$

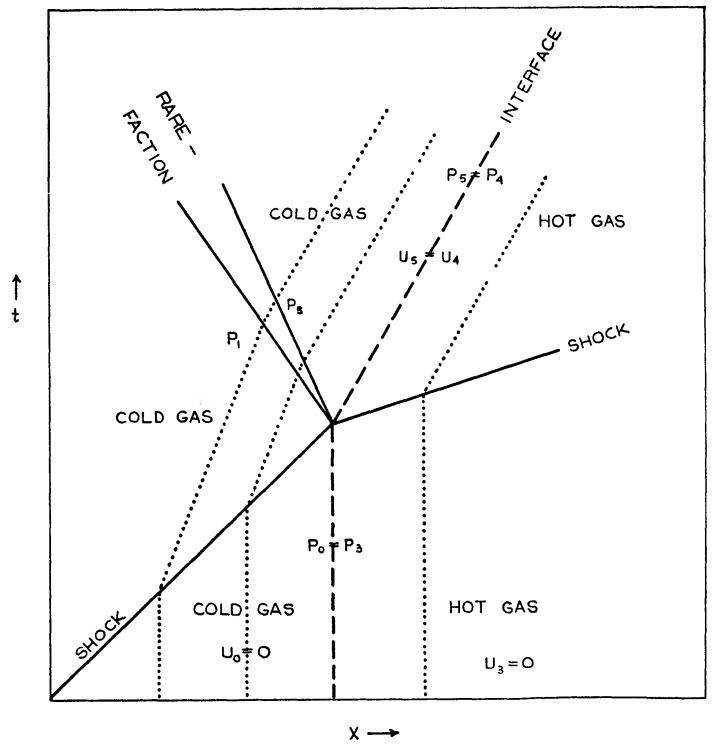

FIG. 5.—x-t diagram of a gas-dynamic shock wave passing from a cold gas (chromosphere) to a hot gas (corona) and exciting a rarefaction wave running back into the cold gas. Shock discontinuities and rarefaction boundaries shown as solid lines, particle paths as dotted line, the boundary between the hot and the cold gas, across which the pressure and velocity are continuous, shown as a dashed line.

Note that we have here written the velocities of sound V_S in the various regions V_0, $V_1, \ldots$, and it can be seen that, with V_0 and V_3 known (the initial conditions in the gases at rest), as well as y_{10} (the shock strength in the cooler gas), these six equations can be solved for the six unknowns u_1, u_4, y_{43}, y_{51}, V_1, V_5.

Since the differential-equation solutions of Table 9 show that strong shocks are incident from below, we have carried out one solution of equations (78)–(83) above for a strong shock with $y_{10} = 3.5$ corresponding to $u_1 = 9.1$ km/sec, $u_1/V_S = 0.76 \approx \bar{\eta}_S$, and the result is $u_4 = 19.5$ km/sec, the velocity of the interface (which we identify with the top of the spicule) up into the corona. This is in the range of velocities of observed spicules, which have a broad distribution with a maximum around 20 or 30 km/sec (Rush and Roberts 1954; Lippincott 1957). Furthermore, for this solution, $V_1 = 15.9$ km/sec, which indicates that the material behind the front is heated by a factor slightly less than 2 before it reaches the top of the chromosphere, while $V_5 = 12.9$ km/sec, which indicates that the expansion as it enters the corona cools the spicular material to a temperature close to that of the top of the average chromosphere. Thus many of the observed properties of the spicules can be understood from the theoretical picture that they are the visible effects of slow-mode shocks. One fundamental difficulty remains, however, namely, that we have completely omitted gravity from our treatment of the waves, although we have used the observed structure of the chromosphere and corona that is ultimately a result of the sun's gravitational field. Therefore, though these ideas should correctly give the initial velocity of a spicule, they do not explain how the spicules can continue to rise for times as long as 5 minutes, reaching heights of 4000 km or more above the chromosphere (Rush and Roberts 1954; Lippincott 1957) in spite of the deceleration of gravity, which would limit their heights to about 1000 km (for an initial velocity of 20 km/sec) on the absence of continuing source of energy. However, a combination of a somewhat stronger shock with a long wave behind it may be sufficient to explain all the observational data, and we may perhaps adopt this picture of spicules as a working model for the time being.

Finally, we discuss briefly the heating of the corona. The integrations of Tables 8 and 9 indicate that the supply of energy carried by the fast and slow shocks is insufficient to supply the coronal losses, which were estimated in Section II to be probably about 1×10^5 ergs/cm^2 sec at sunspot minimum, possibly larger by a factor of 3, possibly smaller by a factor of 10. Therefore, the main source of heating of the corona must be the dissipation of Alfvén waves, a conclusion many previous authors have reached (Alfvén 1947; Piddington 1956; Parker 1958). We have seen in Section VI that these waves cannot penetrate up through the photosphere, so they must be generated in the chromosphere, presumably by the same processes as those discussed above that also generate slow disturbances. The supply of energy in Alfvén waves incident at the top of the chromosphere must be larger than the amount dissipated in the corona, because a considerable fraction is refracted back down without entering the corona. This can be estimated quantitatively if we again idealize the transition as a sharp interface, normal to the magnetic field, because across such a boundary the ratio R of transmitted to incident energy can be found to be

$$R = \frac{4\,(\rho_U/\rho_L)^{1/2}}{[1 + (\rho_U/\rho_L)^{1/2}]^2} \tag{85}$$

from the amplitude relations derived by Roberts (1955), where ρ_U and ρ_L stand for the densities in the upper and lower media, corona and chromosphere, respectively, in our case, with the wave incident from below. For the case of the corona-chromosphere transition, $\rho_U/\rho_L = \frac{1}{100}$ about, so $R = \frac{1}{3}$ about. Thus, to deliver 10^5 ergs/cm^2 sec of energy to the corona in the Alfvén mode required that about 3×10^5 ergs/cm^2 sec be incident from below. This is a rather large amount, considerably greater than the energy that must be put into the slow mode to explain the heating of the upper chromosphere. It can conceivably occur, lower down in the chromosphere, as a consequence of the same processes

that generate the slow-mode disturbances, but again a quantitative calculation is not possible at the present time. Excess heating above plages can certainly be understood as a consequence of excess generation of fast-mode disturbances by magnetic turbulence in the hydrogen convection zone, leading to excess generation of Alfvén waves in the lower chromosphere. In fact, according to this picture, a considerable amount of coronal heating should be due to the plages, and variations in the X-ray and Lyman-α flux would be expected through the solar cycle.

We have seen in Section VI that the Alfvén disturbances pass freely through the chromosphere, with only very small damping by the Joule and frictional heating processes. No compression is involved in an Alfvén disturbance, and hence there is no excess shock dissipation. Parker (1960) has discussed in detail how Alfvén waves in the corona build up to large perturbation velocities, of the order of the Alfvén velocity itself, which is $V_A = 150$ km/sec for an assumed field $B = 1$ gauss and electron density $N_e = 10^8$ cm^{-3}, and then are dissipated. Hence we shall not discuss this process further, but simply consider that whatever energy enters the corona in the form of wave motion will be dissipated there.

However, one further remark concerning the interpretation of the coronal observations may be made at this point. A discrepancy between the coronal temperature deduced from line-width measurements, about 2×10^6 ° K, and the temperature deduced from the ionization equilibrium, about 6×10^5 ° K, remains with the present best estimated values of the relevant ionization cross-sections (Burgess 1960). But the line profiles measured are those of [Fe x] and [Fe xiv], for which the root-mean-square thermal component of velocity is about 20 km/sec, and this is so small in comparison with the expected velocities in the Alfvén waves that it is quite likely that these non-thermal motions make some contribution to the widening of the profile and thus falsify the derived temperature, even in regions selected to be relatively quiet. The observation that in the cases studied by Pecker, Billings, and Roberts (1954) the relative widths of the Fe x, Fe xiv, and Ca xv lines agreed with the thermal widths at a temperature 3500000° K argues against non-thermal motions, but, as these authors point out, further study of other cases is necessary.

IX. FINAL SUMMARY

It has been seen that the generation of fast-mode disturbances in the hydrogen convection zone, their passage through the photosphere, and their dissipation as shocks and the resulting heating of the lower chromosphere can be approximately understood in a quantitative way. The enhanced heating in plage areas is probably due to excess generation of fast-mode disturbances by turbulent magnetic fields in the upper part of the hydrogen convection zone beneath them. The heating of the upper chromosphere is chiefly due to slow-mode shocks, and the spicules observed at the limb are probably chromospheric material pushed up into the corona by these disturbances. The corona is probably heated mostly by Alfvén waves, but the flux required is fairly large if the solar Lyman-α line is emitted in a high-temperature transition zone, with energy provided by conduction of heat inward from the corona. Though Alfvén- and slow-mode waves would be completely absorbed in the photosphere, small-amplitude fast-mode waves are not appreciably dissipated in the chromosphere by Joule heating or frictional heating processes.

More precise estimates of the effects of the slow- and Alfvén-mode waves could be made if their rate of generation were known, but the physical theory for calculating these rates is not at present available. Therefore, a theoretical study of the interaction between two colliding fast shocks, as well as of the mixing of modes caused by the passage of a fast shock through a region with a relatively steep density gradient, is necessary for further quantitative understanding of the outer solar atmosphere. Other complicating effects that have been ignored here but which must be taken into account in a more detailed treatment of the waves in the sun include the preheating of the material ahead of the

shock by radiation excited in the shock and the ionization energy absorbed by material passing through the shock, so the real problem is very complicated indeed, and considerable effort will be required to reach a complete solution.

I should like to express my gratitude to Dr. J. R. Oppenheimer for his kind hospitality extended to me at the Institute for Advanced Study. I am greatly indebted to Drs. R. F. Christy, M. Schwarzschild, B. Strömgren, T. D. Wilkerson, and L. Woltjer for helpful discussions and suggestions on the subjects of this paper and to the John S. Guggenheim Foundation, the Institute for Advanced Study, and the University of Wisconsin Graduate School for support of this research.

REFERENCES

Aboud, A., Behring, W. E , and Rense, W. A. 1959, *Ap. J* , **130,** 381.
Alfvén, H 1947, *M.N.*, **107,** 211.
Ambartsumyan, V. A. 1958, *Theoretical Astrophysics,* trans J B Sykes (London: Pergamon Press), chaps 19, 21.
Athay, R. G , Billings, D. E., Evans, J. W., and Roberts, W. O. 1954, *Ap. J.*, **120,** 94.
Athay, R. G , and Menzel, D H. 1956, *Ap J.*, **123,** 285.
Athay, R. G., and Thomas, R. N. 1956, *Ap. J.*, **123,** 309.
———. 1957, *ibid.*, **125,** 788.
Babcock, H. W., and Babcock, H. D. 1955, *Ap. J.*, **121,** 349.
———. 1958, *International Astronomical Union Symposium No 6: Electromagnetic Phenomena in Cosmical Physics,* ed. B. Lehnert (Cambridge: Cambridge University Press), p. 239
Bates, D. R , Ledsham, K , and Stewart, A. L. 1953, *Phil. Trans. R. Soc. London, A,* **246,** 215.
Bazer, J , and Ericson, W. B. 1959, *Ap. J* , **129,** 758
Bazer, J., and Fleischman, O. 1959, *Phys. of Fluids,* **2,** 366.
Berthold, W. K., Harris, A K., and Hope, H. J. 1960, *J. Geophys. Res.*, **65,** 2233.
Biermann, L. 1948, *Zs f. Ap* , **25,** 161.
Burgess, A 1960, *Ap J.*, **132,** 503.
Chandrasekhar, S 1938, *Stellar Structure* (Chicago: University of Chicago Press), chap 7.
Cillié, G 1932, *M.N* , **92,** 820
Clearman, H E 1953, *Ap. J.*, **117,** 29.
Courant, R , and Friedrichs, K. O 1948, *Supersonic Flow and Shock Waves* (New York: Interscience Publishers, Inc.).
Cowling, T. G. 1945, *M N* , **105,** 166.
———. 1953, *The Sun,* ed G. P Kuiper (Chicago: University of Chicago Press), chap. 8.
——— 1957, *Magnetohydrodynamics* (New York: Interscience Publishers Inc.), chap. 5
Dalgarno, A , and Yadav, H. N. 1953, *Proc Phys Soc. London, A,* **66,** 173.
Daniels, F. B., Bauer, S B , and Harris, A. K. 1960, *J. Geophys. Res* , **65,** 1848.
Dungey, J. W. 1958, *Cosmic Electrodynamics* (Cambridge: Cambridge University Press), pp. 74–75.
Edmonds, F. N , Jr. 1957, *Ap. J.*, **125,** 535.
Ferraro, V. C. A , and Plumpton, C. 1958, *Ap. J.*, **127,** 495.
Friedman, H. 1959, *J. Geophys Res* , **64,** 1751.
———. 1960, *Physics of the Upper Atmosphere,* ed. J A. Ratcliffe (New York: Academic Press, Inc.), chap iv.
Giovanelli, R , 1949, *M N.*, **109,** 358.
Gold, T , 1955, *M.N* , **115,** 340
Goldberg, L , Mohler, O C , and Muller, E A 1959, *Ap. J.*, **129,** 119.
Grad, H , 1959, *Magnetodynamics of Conducting Fluids,* ed. D. Bershader (Stanford: Stanford University Press), p. 37.
Hinteregger, H E , Damon, K. R., Heroux, L R , and Hall, L. A. 1960, *Space Research, Proc. of the First Int. Space Sci. Symposium, Nice,* ed H Kallmann Bijl (Amsterdam: North Holland Publishing Co), p. 615.
Howard, R. 1959, *Ap J.*, **130,** 193
Hulst, H. C. van de 1951, *Problems of Cosmical Aerodynamics* (Dayton: Central Air Documents Office), chap. vi.
———. 1953, *The Sun,* ed G. P Kuiper (Chicago: University of Chicago Press), chap. 5.
——— 1957, *Light Scattering by Small Particles* (New York: John Wiley & Sons, Inc), pp 85–91.
Jager, C. De. 1955, *Ann géophys.*, **11,** 330.
———. 1957*a*, *B A.N.*, **13,** 133
———. 1957*b*, *ibid* , p. 275.
———. 1959*a*, *Nuovo Cimento Suppl.*, Ser. 10, **13,** 291.
———. 1959*b*, *Hdb. d. Phys.*, ed S. Flügge (Berlin: Springer Verlag), **52,** 80.

Johnson, F S , Purcell, J D , Tousey, R , and Wilson, N , 1953, *Ap. J.*, **117,** 238.
Keller, J. B , 1954, *J. Appl Phys* , **25,** 938.
Kulsrud, R M., 1955, *Ap J.*, **121,** 461.
Lamb, H. 1954, *Hydrodynamics* (6th ed.; New York: Dover Publications), sec. 280.
Lehnert, B 1959, *Nuovo Cimento Suppl* , Ser. 10, **13,** 59.
Leighton, R B 1959, *Ap. J.*, **130,** 366.
Lighthill, M. J., 1952, *Proc. R. Soc. London, A* , **211,** 564.
———. 1954, *ibid* , **222,** 1.
———. 1958, *Surveys in Mechanics*, ed. G. K. Batchelor and R M. Davies (Cambridge: Cambridge University Press), p. 250.
———. 1960, *Phil Trans. R Soc. London, A.*, **252,** 397.
Lippincott, S L , 1957, *Smithsonian Contr. Ap* , **2,** 15.
Marshall, W. 1955, *Proc R Soc. London, A*, **233,** 367
Meecham, W. C., and Ford, G W 1958, *J Acoust Soc America*, **30,** 318
Minnaert, M , 1953, *The Sun*, ed G. P. Kuiper (Chicago: University of Chicago Press), chap 3.
Mohler, O , 1951, *M.N* , **111,** 630.
Morton, D. C., and Widing, K. G. 1960*a*, *Ann d'ap* , **23,** 968.
——— 1960*b*, *A.J.*, **65,** 58.
Osterbrock, D. E., 1952, *Phys. Rev* , **87,** 468.
Parker, E. N. 1953, *Ap. J.*, **117,** 431.
———. 1958, *ibid.*, **128,** 677.
———. 1960, *ibid.*, **132,** 821.
Pecker, C , Billings, D. E , and Roberts, W O. 1954, *Ap J* , **120,** 509
Piddington, J. H., 1956, *M.N.*, **116,** 314
——— 1958, *International Astronomical Union Symposium No 6: Electromagnetic Phenomena in Cosmical Physics*, ed B. Lehnert (Cambridge: Cambridge University Press), p. 141.
Proudman, I 1952, *Proc R Soc London, A*, **214,** 119
Purcell, J D , Packer, D. M , and Tousey, R 1960, *Space Research, Proc of the First Int Space Sci Symposium, Nice*, ed. H Kallmann Bijl (Amsterdam: North Holland Publishing Co), p. 594
Roberts, W O 1945, *Ap J.*, **101,** 136
Rogerson, 1961, J B Jr., in preparation.
Rush, J H , and Roberts, W O. 1954, *Australian J. Phys* , **7,** 230.
Schatzman, E. 1949, *Ann d'ap* , **12,** 203.
Schirmer, H. 1950, *Zs f Ap* , **27,** 132.
Schwarzschild, M 1948, *Ap. J* , **107,** 1.
Smith, E v P 1960, *Ap J* , **132,** 202.
Sommerfeld, A 1950, *Mechanics of Deformable Bodies* (New York: Academic Press, Inc), sec 37.
Spiegel, E A 1957, *Ap J.*, **126,** 202
Spitzer, L., Jr 1958, *International Astronomical Union Symposium No. 6: Electromagnetic Phenomena in Cosmical Physics*, ed B. Lehnert (Cambridge: Cambridge University Press), p 169
Thomas, R N. 1948, *Ap. J* , **108,** 130.
Vitense, E. 1953, *Zs f. Ap* , **32,** 135.
Weymann, R 1960, *Ap. J.*, **132,** 452
Weymann, R., and Howard, R. 1958, *Ap J.*, **128,** 142
Wilson, O C , and Bappu, M. K. V. 1957, *Ap. J.*, **125,** 661.
Woltjer, L 1954, *B A N* ,**12,** 165.
Woolley, R v d R , and Allen, C. W. 1950, *M.N* , **110,** 358.
Wurm, K. 1948, *Zs f Ap* , **25,** 109.